Ship Frame Research Program: a numerical study of the capacity of single frames subject to ice load

Pavic, M.; Daley, C.; Hussein, A.; Hermanski, G.

Publisher's version / Version de l'éditeur:
https://doi.org/10.4224/8896087
Technical Report; no. TR-2004-04, 2004

DOCUMENTATION PAGE

REPORT NUMBER	NRC REPORT NUMBER	DATE
TR-2004-04		February 2005
REPORT SECURITY CLASSIFICATION		**DISTRIBUTION**
Unclassified		Unlimited

TITLE

SHIP FRAME RESEARCH PROGRAM-

A Numerical Study of the Capacity of Single Frames Subject to Ice Load

AUTHOR(S)

[1]Mihailo Pavic, [1]Claude Daley, [1]Amgad Hussein

[2]Greg Hermanski

CORPORATE AUTHOR(S)/PERFORMING AGENCY(S)

[1]Ocean Engineering Research Center, Memorial University of Newfoundland, St. John's, NL

[2]Institute for Ocean Technology, National Research Council, St. John's, NL

PUBLICATION

SPONSORING AGENCY(S)

Ocean Engineering Research Center, Memorial University of Newfoundland, St. John's, NL

Institute for Ocean Technology, National Research Council, St. John's, NL

IOT PROJECT NUMBER	NRC FILE NUMBER		
42_987_16			
KEY WORDS	**PAGES**	**FIGS.**	**TABLES**
ship frames, instabilities, deformation	iv, 32	36	6

SUMMARY

This report presents results of a finite element analysis of ship frames subject to ice loads. The analysis covers the full range of frame behavior, from elastic, through yield, through the formation of initial mechanisms, through large deformations. The behaviors often include some local instabilities (buckling). The analyses continue until the total central deformation reaches about 10% of the frame span. The parameters include:

- frame profile: Angle, Tee, Flat
- frame span:
- load length: patch (trans.), uniform (long'l)
- web thickness:
- flange thickness:
- end brackets: with, without

The ANSYS finite element program was used in this study [1].

The aim of the study is to determine the validity of the limit state equation employed in the IACS new Unified Requirements for Polar Ships [2]. In particular, the study focuses on the reasons why some frames may not behave in accordance with the limit state equations, with local buckling and tripping as key issues. The report builds upon the work presented in [3].

In the present draft of the UR, there are no explicit tripping requirements. There are local buckling requirements, though they are essentially the same local buckling requirements employed widely in classification requirements for open water ships. This report examines the possible need for tripping requirements in the Polar Rules and the possible need for changes to the local bucking requirements.

ADDRESS National Research Council
Institute for Ocean Technology
Arctic Avenue, P. O. Box 12093
St. John's, NL A1B 3T5
Tel.: (709) 772-5185, Fax: (709) 772-2462

National Research Council Canada
Institute for Ocean Technology

Conseil national de recherches Canada
Institut des technologies océaniques

SHIP FRAME RESEARCH PROGRAM-

A NUMERICAL STUDY OF THE CAPACITY OF SINGLE FRAMES SUBJECT TO ICE LOAD

TR-2004-04

Mihailo Pavic, Claude Daley, Amgad Hussein
Greg Hermanski

March 2004

OERC Report 2004-02
IOT Report TR-2004-04

Ship Frame Research Program-
A Numerical Study of the Capacity of Single Frames Subject to Ice Load

March 20, 2004

By

Mihailo Pavic, Claude Daley, Amgad Hussein
Ocean Engineering Research Center
Memorial University of Newfoundland

and

Greg Hermanski
Institute for Ocean Technology
National Research Council of Canada

Memorial
University of Newfoundland

National Research Council Canada
Conseil national de recherches Canada

TABLE OF CONTENTS

SYMBOLS AND NOTATION

IACS	International Association of Classification Societies
a	length of shear panel
Af	area of the flange
Aw	area of the web
b	height of the ice load patch
hw	height if the web
kw	area ratio
kz	ratio of zp to Zp
L	length of frame
P_{3h}	pressure causing collapse for case of 2 fixed supports
Ps	pressure causing collapse for end load case
S	frame spacing
tw	thickness of web
Zp	plastic section modulus
zp	sum of plastic section moduli of plate and flange
Zpns	a non-dimensional modulus
σ_y	yield stress
L1800nb_W11/308_P20_F16/95	This refers to an L section frame, 1800mm long, with a Web 11mm thick, 308mm high, with 20mm shell Plate, and a 16 by 95mm Flange.

TABLE OF FIGURES

TABLE OF TABLES

Acknowledgement

The work was made possible with the support of funding from a number or organizations sponsoring this research program. These include Transport Canada, Defense Research and Development Canada (Atlantic), the US Coast Guard, and the member agencies of the Ship Structures Committee. In particular we acknowledge the input and support from Mr. Jacek Dubiel (TC), Mr. Dave Stredulinsky (DRDC) and Mr. Alfred Tunik (USCG).

1 Introduction

This report presents results of a finite element analysis of ship frames subject to ice loads. The analysis covers the full range of frame behavior, from elastic, through yield, through the formation of initial mechanisms, through large deformations. The behaviors often include some local instabilities (buckling). The analyses continue until the total central deformation reaches about 10% of the frame span. The parameters include:

- frame profile: Angle, Tee, Flat
- frame span:
- load length: patch (trans.), uniform (long'l)
- web thickness:
- flange thickness:
- end brackets: with, without

The ANSYS finite element program was used in this study [1].

The aim of the study is to determine the validity of the limit state equation employed in the IACS new Unified Requirements for Polar Ships [2]. In particular, the study focuses on the reasons why some frames may not behave in accordance with the limit state equations, with local buckling and tripping as key issues. The report builds upon the work presented in [3].

In the present draft of the UR, there are no explicit tripping requirements. There are local buckling requirements, though they are essentially the same local buckling requirements employed widely in classification requirements for open water ships. This report examines the possible need for tripping requirements in the Polar Rules and the possible need for changes to the local bucking requirements.

2 Background

The Ocean Engineering Research Center and the Institute for Ocean Technology are conducting a research program to study the plastic behavior and ultimate limit states of ship frames and grillages subject to lateral loads. This work is closely related to the development of the new IACS Unified Requirement for Polar Ship Construction. The Polar Rules contain limit state equations for ship frames subject to lateral loads (ice loads)[3]. The limit state equations were derived on the basis of energy methods (plastic work)[4]. This research program is aimed at validating the limit state equations for single frames, determining any limits to the validity, and exploring the way frames interact in grillages. The problem under study also applies to cases of hydrodynamic impact and other types of collisions. As a result, the research applies to most ship structures and many types of offshore structures.

The program consists of several experimental phases (see Figure 1), each supported by numerical investigations. The first phase is the testing of a variety of single frames. The second phase is the testing of a grillage of three frames (small grillage). The third phase is the testing of a grillage of nine frames (large grillage).

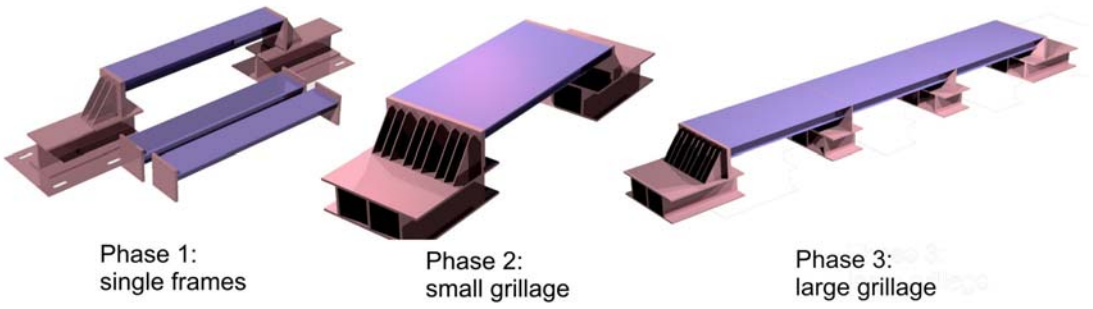

Figure 1. The three experimental phases in the ship frame research program

The three experimental phases support each other in important ways. Ships frames are always part of a structural system (a grillage). However, design and regulation normally consider single frames. The UR limit state equations were derived by considering a single frame in isolation.

The first phase of the experiments will focus on the single frame in isolation and will attempt to assess the validity of the UR equations. The UR contains a set of requirements that are based on 2 distinct limit states. The UR contains a formula for the required minimum shear area and the required modulus. The required modulus is greatest for the case of the shear area being at the minimum. If the shear area is greater than the minimum, then the required modulus is less. In this way the interaction between bending and shear is accounted for. These are explained in [4,5,6]. Also given are related capacity equations that give the patch pressure that will cause the limit state to occur in both 3 hinge bending (for a central load), and end shear collapse (for an end load). Equation (1) gives the central load capacity value. The terms are defined in the nomenclature. A full explanation is given in [4,5]. Only central load cases are analyzed in this report. Equation (1) is used to give the UR value ("UR formula") in the analysis. It is also the normalizing pressure for many of the plots.

$$P_{3h} = \frac{(2-kw)+kw\cdot\sqrt{1-48\cdot Zpns\cdot(1-kw)}}{12\cdot Zpns\cdot kw^2+1}\cdot\frac{Zp\cdot\sigma_y\cdot 4}{\left[S\cdot b\cdot L\cdot\left(1-\frac{b}{2\cdot L}\right)\right]} \quad (1)$$

In the second experimental phase of the program, the frames will be part of a small grillage and will have more realistic side boundary conditions. In the third phase the side and end boundary conditions (for the frame in the center) will be the most realistic. All together, we will develop an understanding of the frame behavior and the reasons why there may be deviations from the behavior implicit in the UR equations.

The experimental work will be supported by extensive finite element analysis. This report presents a finite element study of a wide range of single frames.

Figure 2 sketches the typical load deflection pattern that we tend to have in ice strengthened frames. The deflection is the maximum deflection of the web under at the plate-web connection. The UR limit state (equation 1) represents a capacity comparable to that labeled “mechanism 1” in Figure 2. Prior to mechanism 1, the load-deflection curve is essentially linear and follows the slope of the original elastic trend. Yielding occurs well before mechanism 1. This is followed by the expansion of the plastic zone, during which stress redistribution takes place. Once the plastic zone fills one or more critical cross sections, a plastic mechanism forms, allowing large and permanent deformations. Mechanism 1 might be called ‘collapse’, though this term is not exactly correct. Subsequent to mechanism 1, while the frame is ‘collapsing’ in bending, membrane forces tend to rise and support the growing load. Further along this curve, additional mechanisms can occur, including buckling and fracture. In the analyses in this report, some frames experience local buckling after the first mechanism. Ideally the frame would exhibit monotonically increasing capacity, even as the permanent deflections grow very large.

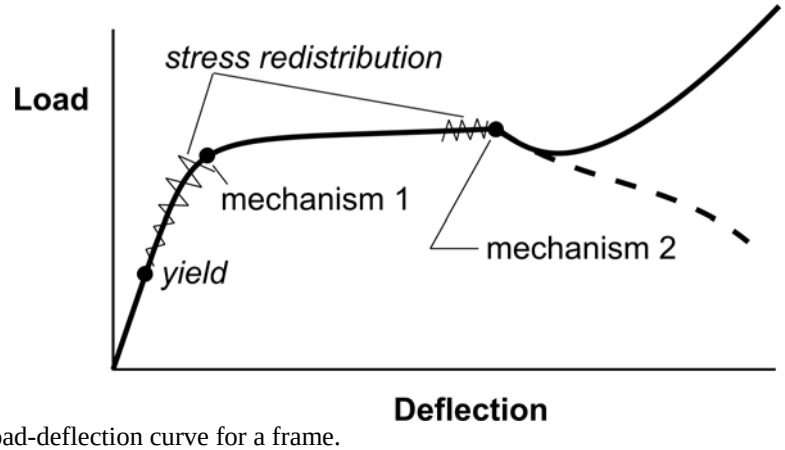

Figure 2. Idealized load-deflection curve for a frame.

3 Finite Element Modeling

The analysis presented here was performed using the finite element analysis program ANSYS [1]. Other than those specifically indicated, shell elements (shell-181) were used to model the frames.

The adopted shell element is suitable for analyzing thin to moderately thick shell structures. It is a 4-node element with all six degrees of freedom at each node: three translations (in the x, y, and z directions), and three rotations (about the x, y, and z-axes).

The element is well suited for linear, large rotation, and/or large strain nonlinear applications. Change in shell thickness is accounted for in the nonlinear analysis. In the element domain, both full and reduced integration schemes are supported. In addition, the element accounts for follower (load stiffness) effects of distributed pressures.

The geometry, node locations, and the coordinate system for this element are shown in Figure 3. The element formulation is based on logarithmic strain and true stress measures. The element kinematics allow for finite membrane strains (stretching) which makes it suitable for the present analysis. However, the curvature changes within a time increment are assumed to be small.

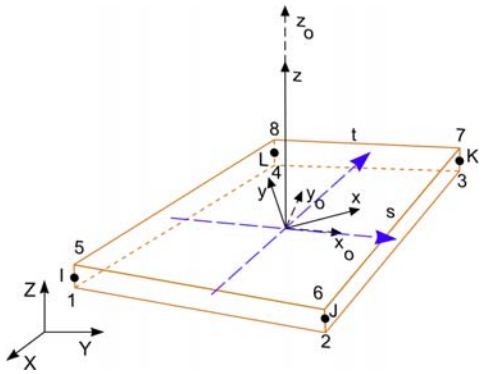

Figure 3. SHELL181 Geometry (from ANSYS help files)

Figure 5 sketches the steps involved in the finite element analysis. These steps can be performed interactively, or by creating a text input file that includes the appropriate commands and data in sequence. Appendix A is a listing of a typical input file. Post processing of the results was performed interactively. The load-deflection data was exported for plotting. The results were extracted and imported in a spreadsheet, and the plots were generated.

A whole frame was modeled rather than one half of a frame with symmetric boundary conditions at the centre of the frame. This type modeling was used to ensure that the model is capable of modeling local buckling at any location of the beam. The edges of the section were constrained to move in the vertical direction only (symmetric boundary). This assumption reflects an actual ship frame with top plate connected at both ends of the section, thus providing some bracing to the top flange. The imposed boundary conditions are shown in Figure 4.

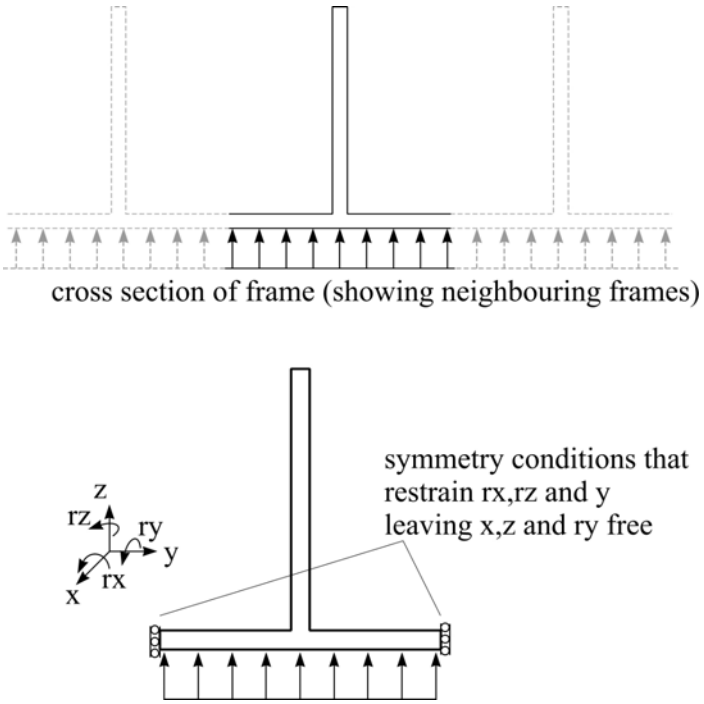

Figure 4. Sketch of the lateral boundary conditions on the frame.

The influences of the element type and material properties were also examined. In addition to the shell elements used, the frames were also modeled using a three-dimensional brick element (ANSYS element solid-92). Brick elements have three translation degrees of freedom at each node. Brick elements provide fairly accurate actual results but they are computer-time consuming. Appendix B presents the results of the two different types of elements: namely shell and brick elements. Also, Figure 34 depicts the results obtained using the two elements. The results show that up to the design point the two models agree very well. In the large deformation region, the brick element model gives higher load values. This tends to show that shells produce a more conservative estimate of capacity. A higher density brick model (i.e. with more than one brick through the thickness) may have given results closer to the shell results.

In order to study the effect of post-yield modulus on the inelastic behaviour of the frame, two values were examined. The two post yield modulus values were 50 MPa and 500 MPa.
The results (Figure 35) indicated that the lower value (50 MPa) gives lower and more conservative results. Consequently, the 50MPa value was used in the analyses presented elsewhere in this report.

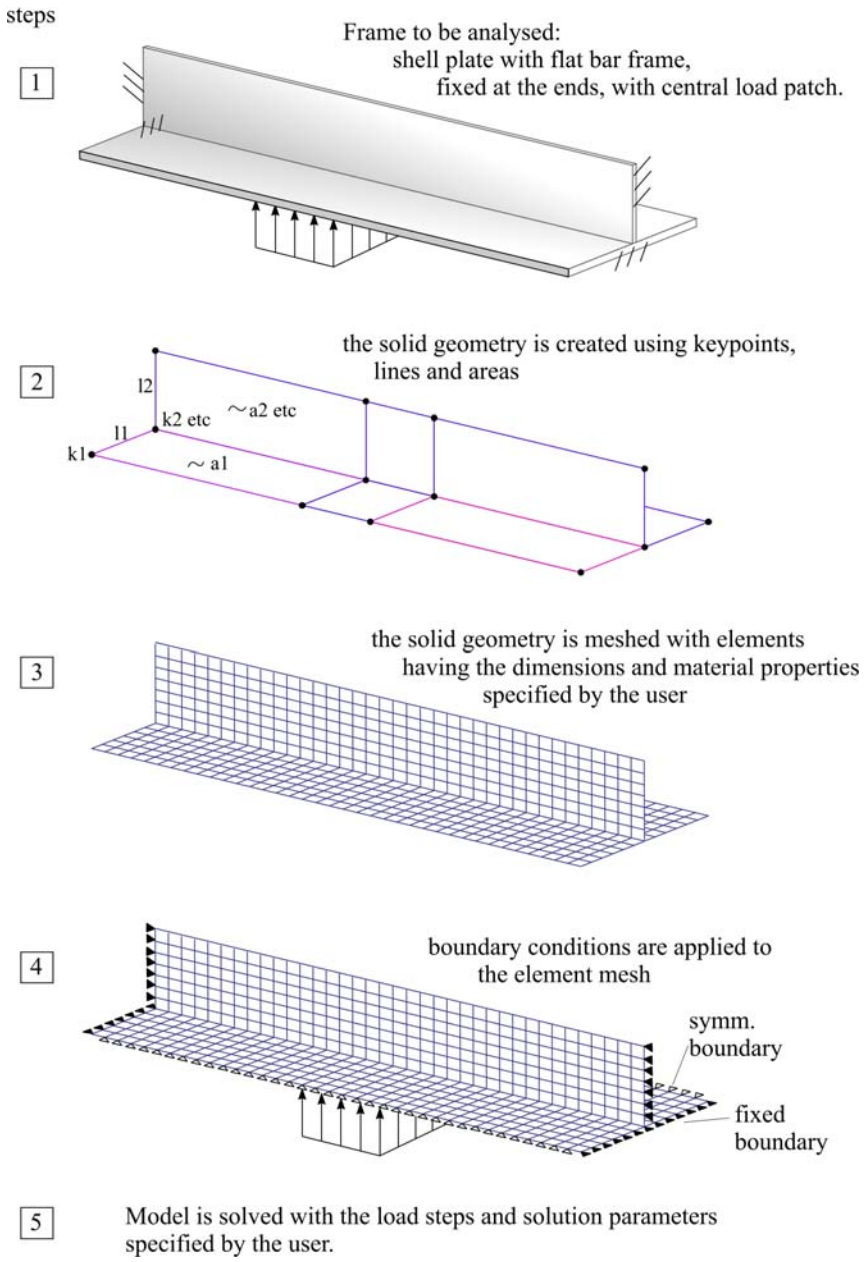

Figure 5. Outline of finite element analysis steps.

4 Longitudinal Frame Analysis

4.1 Analysis Grid

The longitudinal frames shown in Table 1 were all analyzed with a uniform load over the entire span. The main variants were section type, web thickness, frame length and the presence or absence of brackets.

Table 1. Longitudinal frame parameters

Run No.	Section type	Plate thk. [mm]	Web height [mm]	Web thk. [mm]	Flange width [mm]	Flange thk. [mm]	Frame length [mm]	Brackets l x h x t [mm]	hw / tw	805 /$(\sigma_y)^{0.5}$	Capacity by UR formulae (MPa)(eqn 1)
1	L	20	308	11	95	16	2400	300 X 300 X 15	28.0	45.4	1.39
2	L	20	308	11	95	16	1800	no brackets	28.0	45.4	1.62
3	L	20	308	11	95	16	3600	300 X 300 X 15	28.0	45.4	0.93
4	L	20	308	11	95	16	3000	no brackets	28.0	45.4	1.01
5	L	20	308	9	95	16	2400	300 X 300 X 15	34.2	45.4	1.15
6	L	20	308	7	95	16	2400	300 X 300 X 15	44.0	45.4	0.91
7	L	20	308	8	95	16	2400	no brackets	38.5	45.4	0.9
8	T	20	308	11	95	16	2400	300 X 300 X 15	28.0	45.4	1.39
9	T	20	308	11	95	16	1800	no brackets	28.0	45.4	1.62
10	T	20	308	11	95	16	3600	300 X 300 X 15	28.0	45.4	0.93
11	T	20	308	11	95	16	3000	no brackets	28.0	45.4	1.01

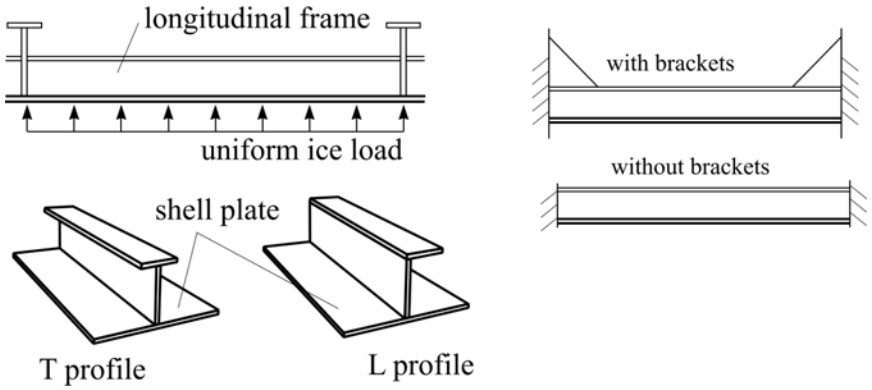

Figure 6. Sketch of longitudinal frame geometry.

4.2 Load-Deflection Results

The load-deflection relationships are the main result of the analysis. The intended successful behavior is to maintain load-bearing capability with minimal permanent deflection. As long as fracture and buckling are avoided, frames can be expected to support load well above the yield point. When the plastic zones grow sufficiently large, local plastic mechanisms form. After this, the plastic deformations grow significantly, while the capacity may either fall or continue to grow. Figure 7 shows a variety the load-deflection plots for the frames in Table 1. Figure 8 shows just the results for the T profiles. Figure 9 shows L sections without brackets. Figure 10 shows L sections with brackets. (Note: the deflection is at the center of the frame, just under the load patch. See the Nomenclature for an explanation of the curve labels.)

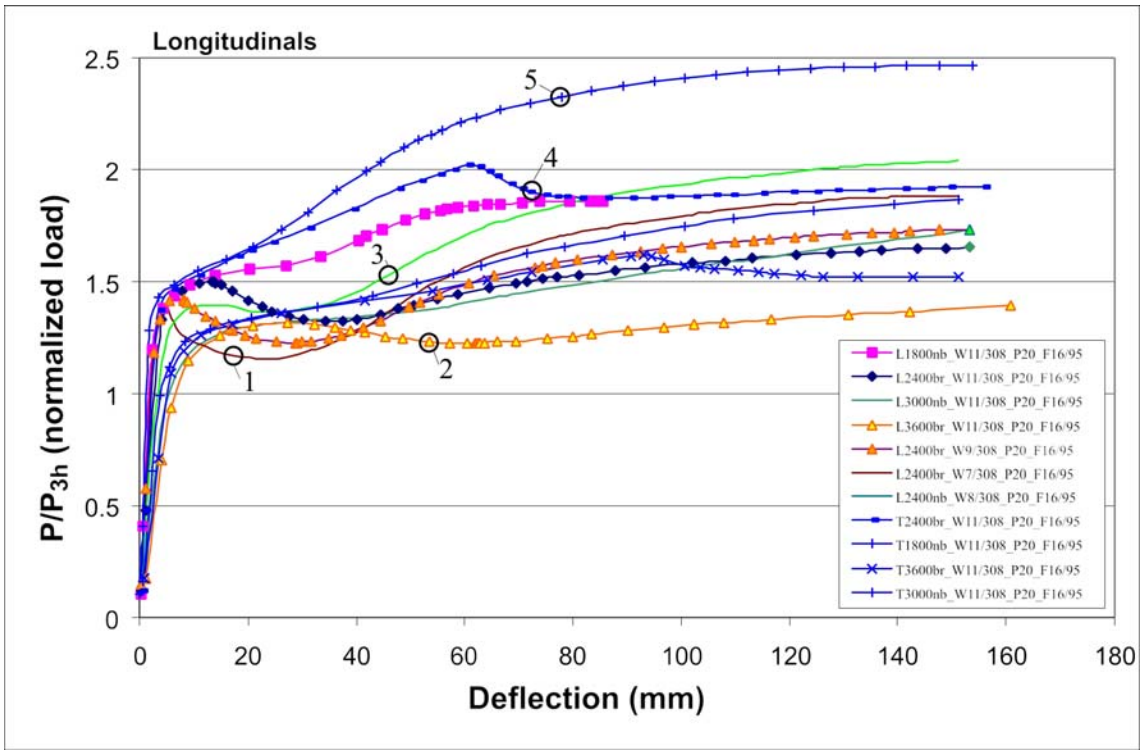

Figure 7. Longitudinal frames: normalized load–deflection curves. Numbered circles represent deformation plots.

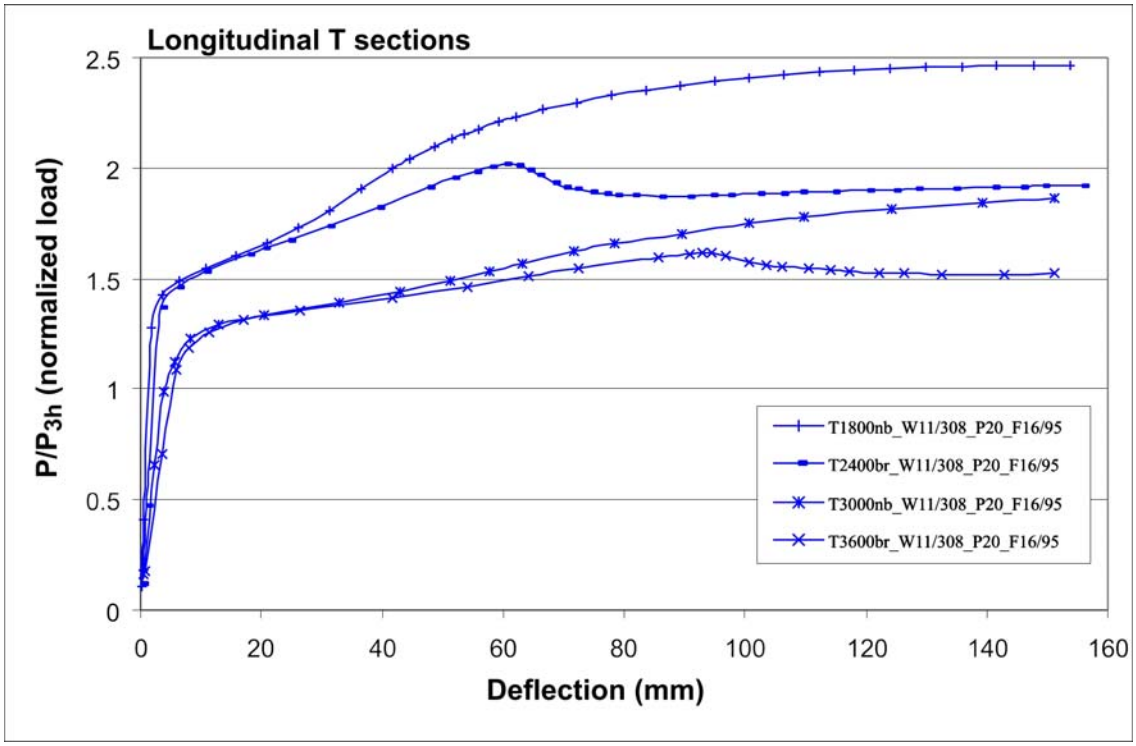

Figure 8. Longitudinal T profiles: normalized load–deflection curves.

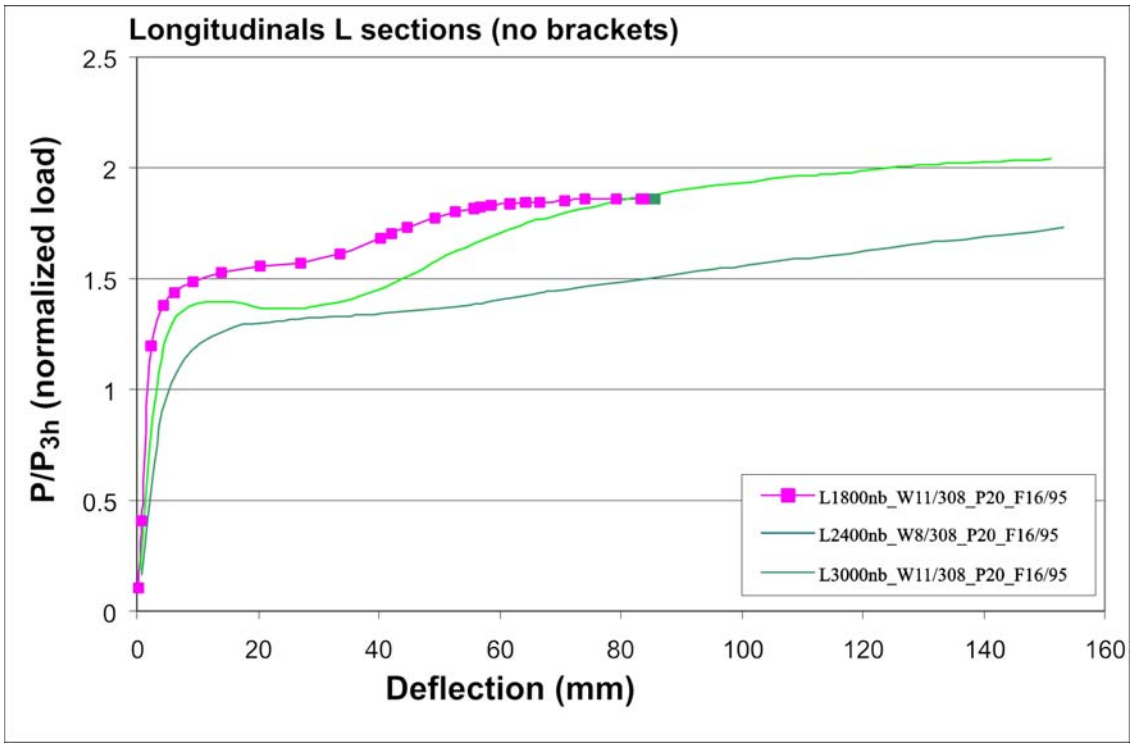

Figure 9. Longitudinal L profiles without brackets: normalized load–deflection curves.

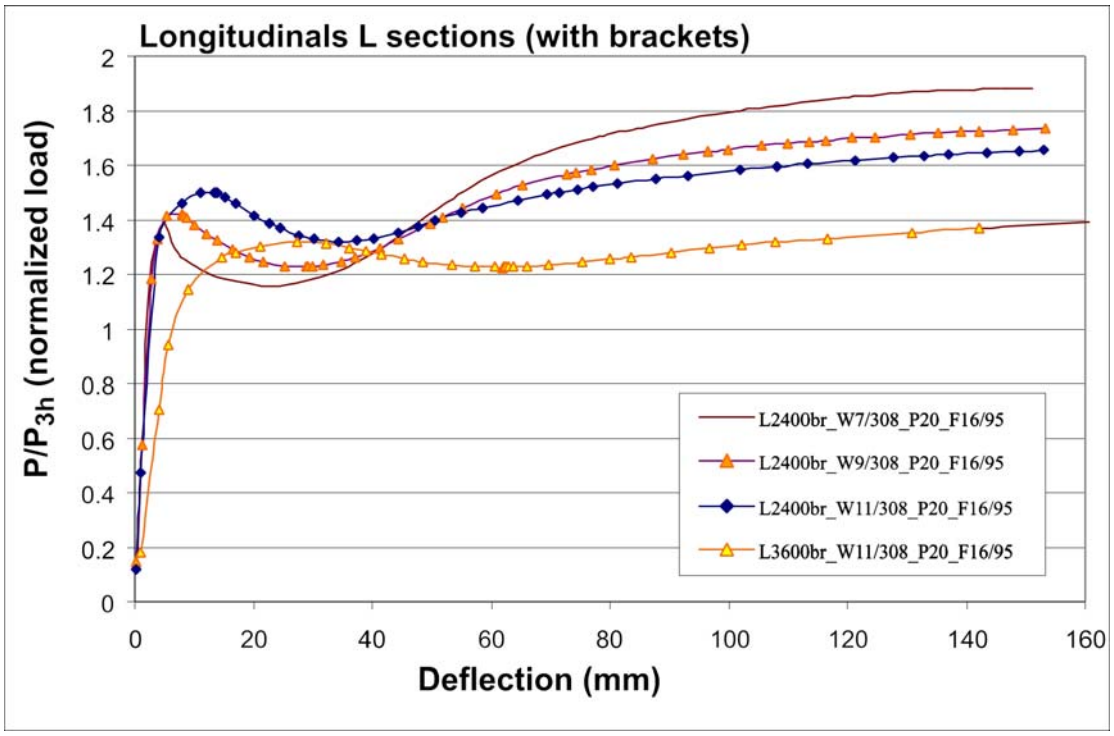

Figure 10. Longitudinal L profiles with brackets: normalized load–deflection curves.

4.3 Deformation Plots

The plots shown below show the deformation pattern at the points indicated by the numbered circles in Figure 7.

Table 2. Table of ANSYS plots (plot number corresponds with circle numbers on the Figure 7 load deflection curves)

Circle No.	Frame type	Frame dimensions (mm)	Frame length (mm)	Load level (MPa)
1	L longitudinal	W 7/308_P 20_F 16/95	2400	1.07
2	L longitudinal	W 11/308_P 20_F 16/95	3600	1.15
3	L longitudinal	W 8/308_P 20_F 16/95	2400	1.27
4	T longitudinal	W 11/308_P 20_F 16/95	2400	2.65
5	T longitudinal	W 11/308_P 20_F 16/95	1800	3.72

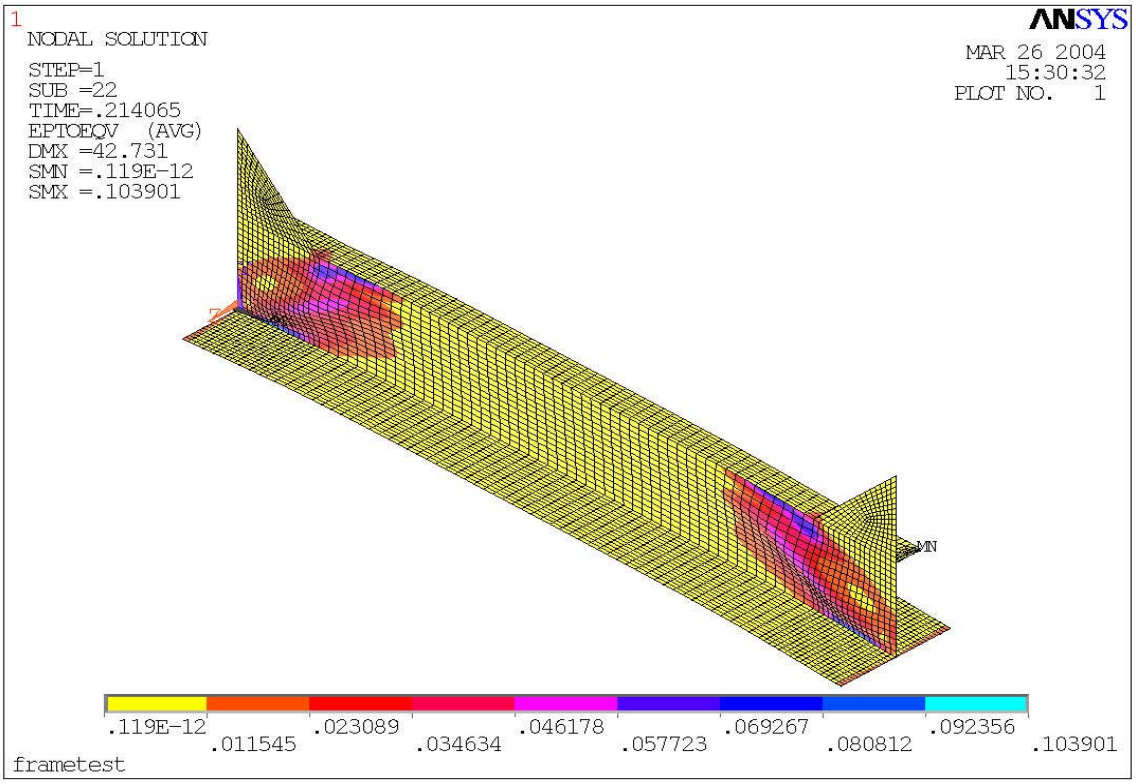

Figure 11. Plot of deformation (with strain contours) for circle #1.

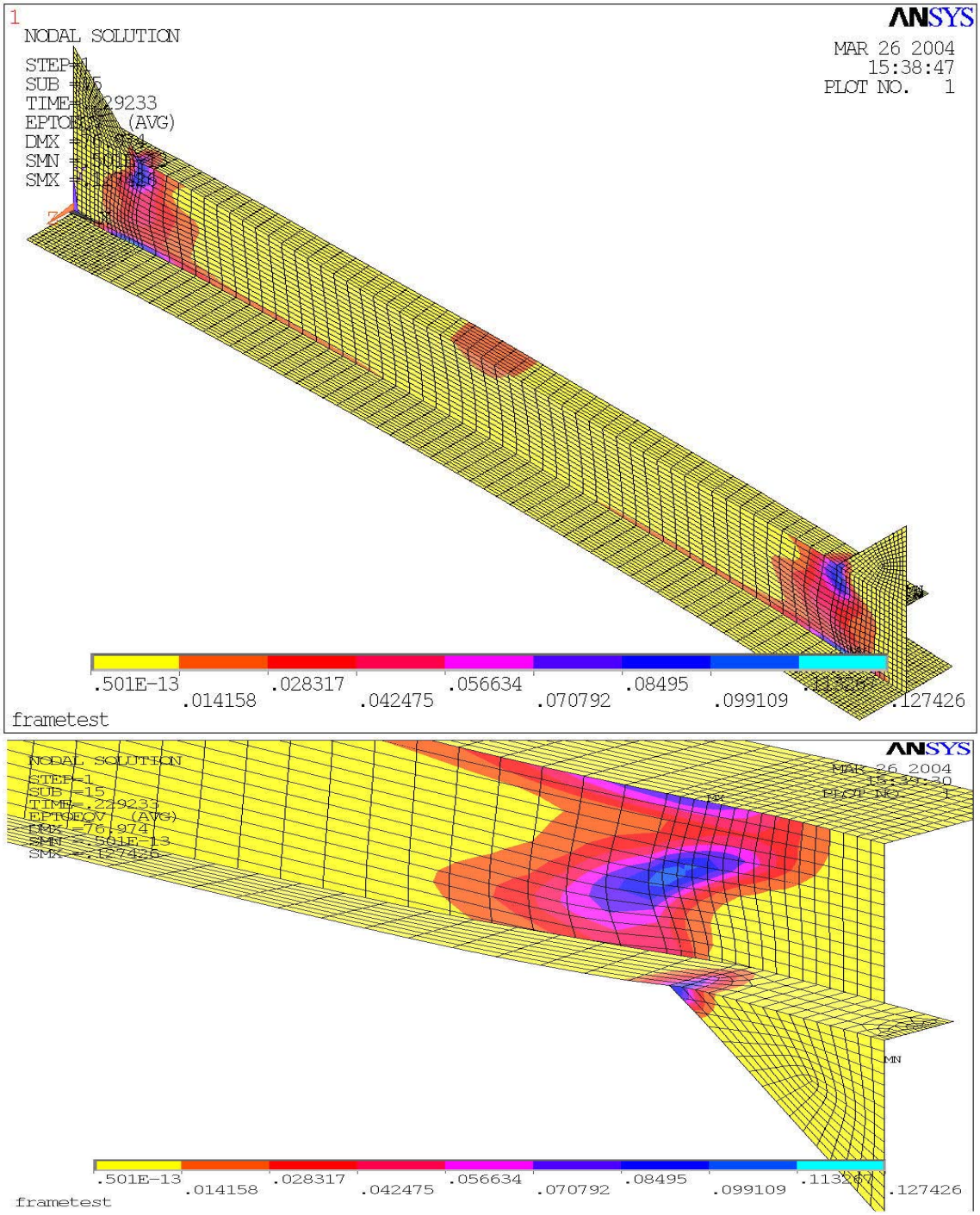

Figure 12. Plot of deformation (with strain contours) for circle #2.

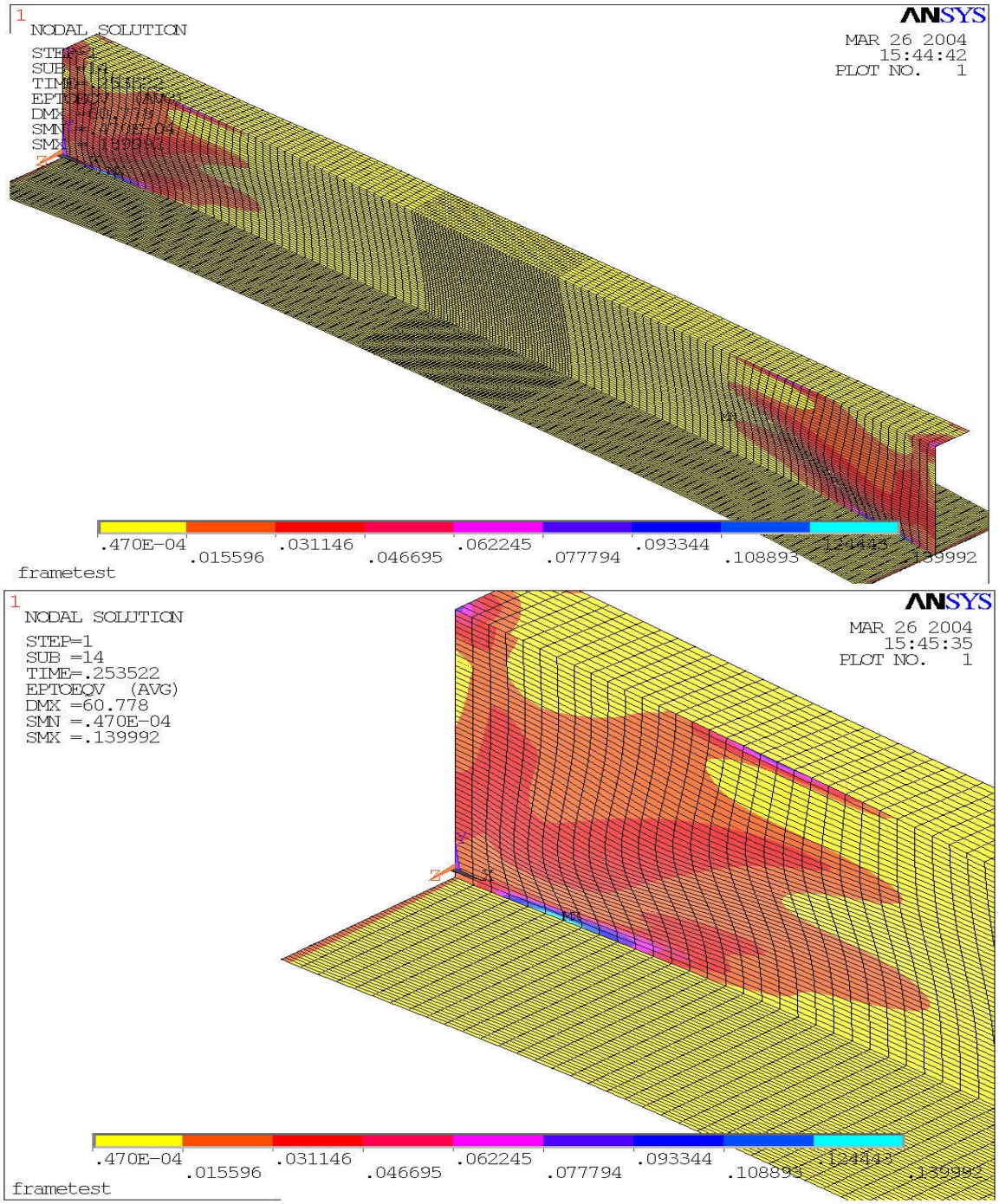

Figure 13. Plot of deformation (with strain contours) for circle #3.

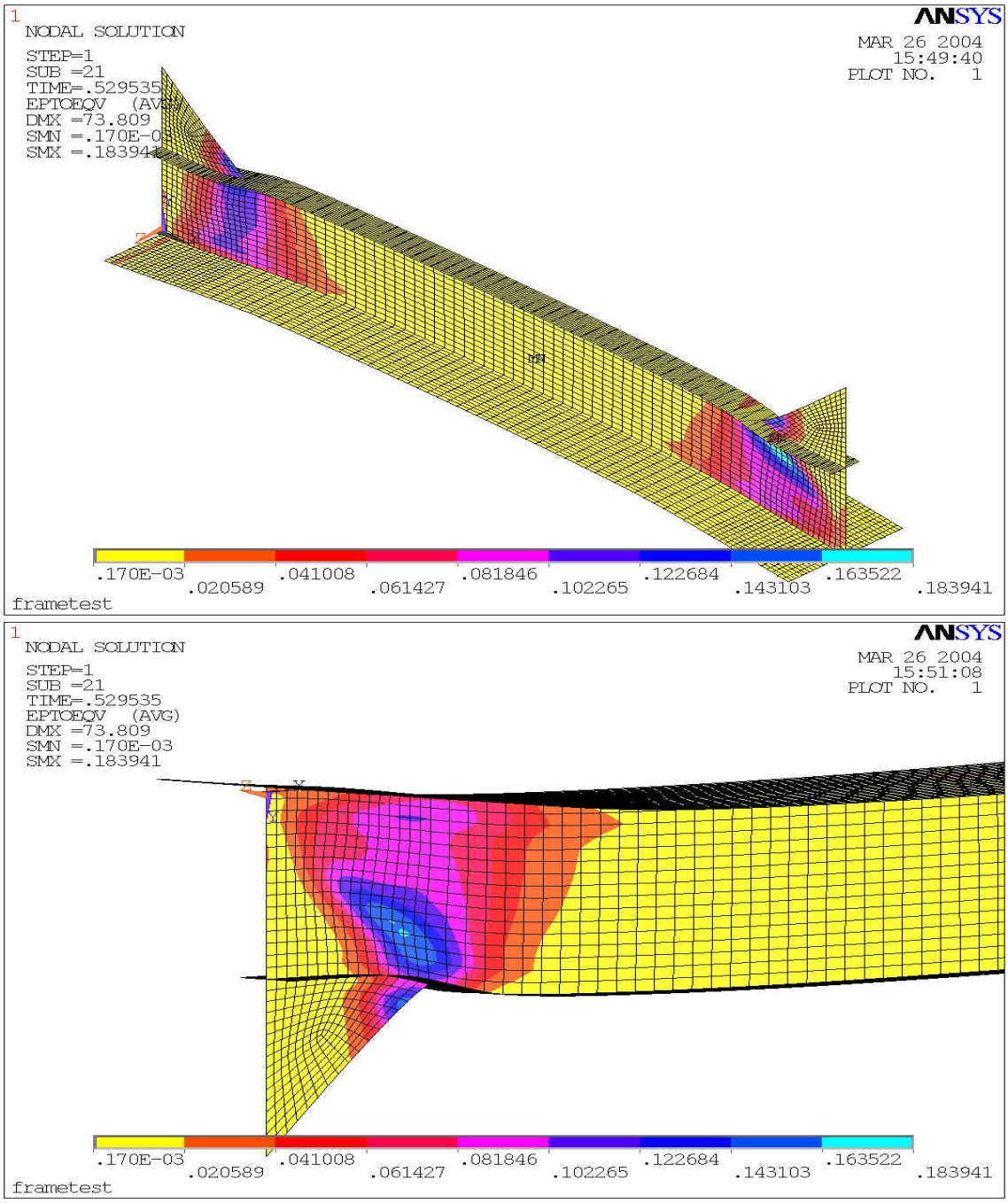

Figure 14. Plot of deformation (with strain contours) for circle #4.

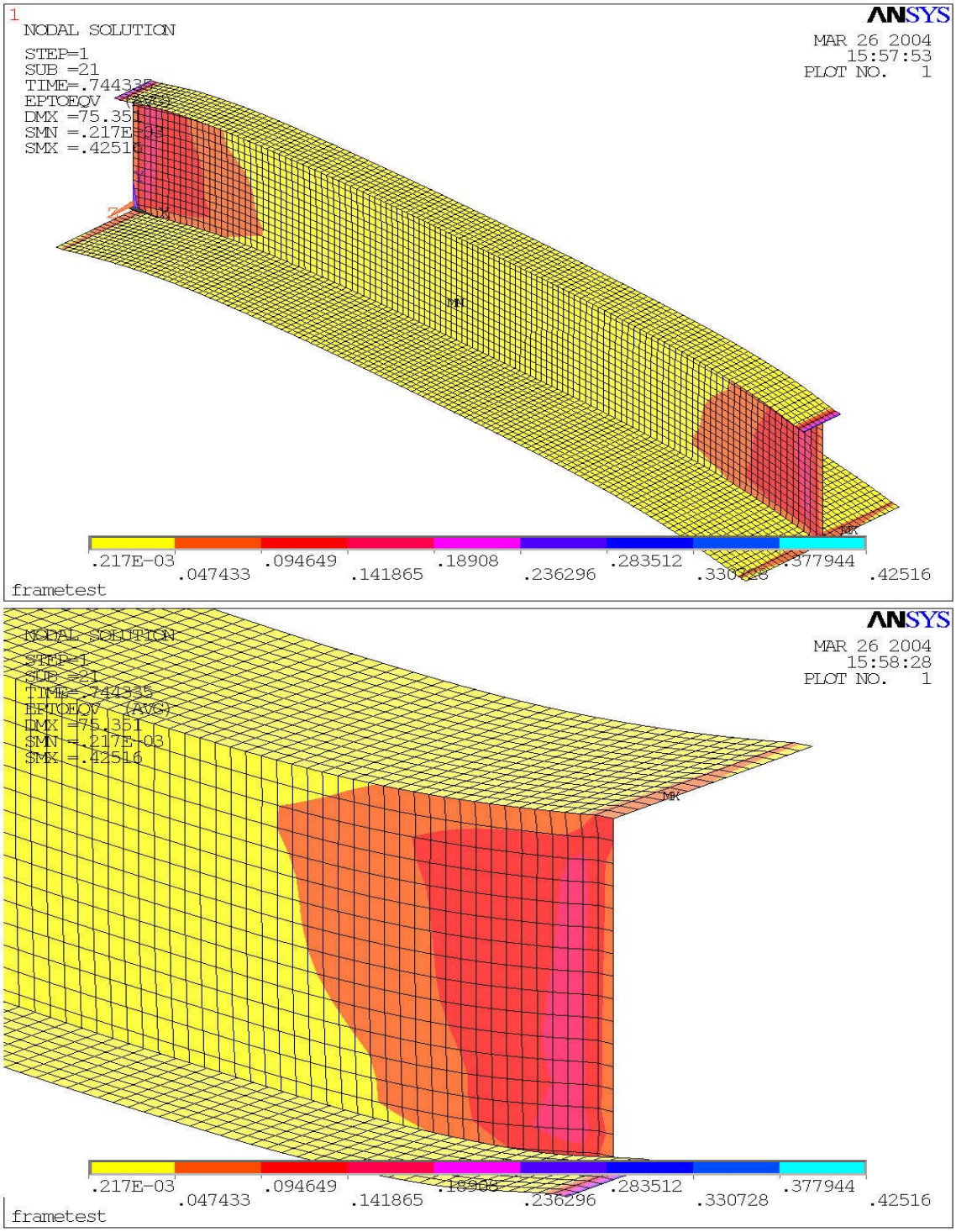

Figure 15. Plot of deformation (with strain contours) for circle #5.

4.4 Discussion of Longitudinal Frame Results

The most obvious result of the longitudinal frame analysis is that all the frames in Table 1 (see Figure 7) have enough capacity to sustain UR formulae design load, and maintain this capacity even at large deformations. The local deformations of the stiffener web under the bracket toe (e.g Figure 12) have no crucial influence on the global stiffener capacity. The small loss of the capacity manifested as slump on the load deflection curves, caused by local web buckling, still leaves a substantial capacity reserve to the stiffener. Those localized deformations seem to be the result of web overloading in shear. Short stiffeners with end bracket fitted are particularly susceptible to this behaviour.

Figure 8 shows just the T profiles and illustrates some interesting trends. The plots give normalized capacity (i.e. capacity relative to the UR limit state intended capacity). Shorter T frames result in higher capacity, though the results do not seem to be smoothly dependant on length. It seems that above a certain length, the capacity falls. This may indicate that a certain behavior occurs in frames longer than a critical value.

Another interesting observations is that, in T frames, while brackets do not appear to affect the initial plastic limit (i.e where the first bend in the load-deflection curve occurs), there is an effect on the reserve behavior. Frames with brackets appear to have a minor load drop, likely indicating a minor instability mechanism.

Figure 9 shows L frames without brackets. As with T frames, there is no sudden change and drop in capacity. The frame with the thinnest web (8mm) did have a slight but smooth lost in capacity after the design point was reached. In addition, similar to T frames, the shorter frames exhibit greater capacity. Asymmetry causes earlier web overloading problems with L sections. In both L and T sections the membrane effects eventually become effective, though only after large localized web deformations.

Figure 10 shows L frames with brackets. Again, there is a similarity with T sections. The frames with thinner webs exhibit a more sudden drop in capacity. The longer frames appear to have a lower design capacity, yet tend not to show any sudden drops in capacity.

5 Transverse Frame Analysis

5.1 Analysis Grid

The transverse frames shown in Table 3 were all analyzed with a patch load length 400mm and breadth equal to stiffener spacing. The main variants were section type, web, plate and flange thickness, frame length and the presence or absence of brackets.

Table 3. Transverse frame parameters

Run No.	Section	Plate thk. [mm]	Web height [mm]	Web thk. [mm]	Flange width [mm]	Flange thk. [mm]	Frame length [mm]	Bracket l x h x t [mm]	hw / tw	805 /$(\sigma_y)^{0.5}$	Capacity by UR formulae (MPa)(eqn 1)
1	L	20	308	11	95	16	2400	300 X 300 X 15	28.0	45	7.21
2	L	20	308	9	95	16	2400	300 X 300 X 15	34.2	45	6.24
3	L	20	308	8	95	16	2400	300 X 300 X 15	38.5	45	5.55
4	L	20	308	7	95	16	2400	300 X 300 X 15	44.0	45	4.78
5	L	20	308	13	95	16	2400	300 X 300 X 15	23.7	45	8.07
6	L	11	308	11	95	16	2400	300 X 300 X 15	28.0	45	7.1
7	L	11	308	11	95	11	2400	300 X 300 X 15	28.0	45	6.28
8	L	20	308	11	95	16	2400	no brackets	28.0	45	6.57
9	L	20	308	11	95	16	2100	no brackets	28.0	45	7.22
10	T	20	308	11	95	16	2400	300 X 300 X 15	28.0	45	7.21
11	T	20	308	9	95	16	2400	300 X 300 X 15	34.2	45	6.24
12	T	20	308	8	95	16	2400	300 X 300 X 15	38.5	45	5.55
13	T	20	308	7	95	16	2400	300 X 300 X 15	44.0	45	4.78
14	T	20	308	13	95	16	2400	300 X 300 X 15	23.7	45	8.07
15	L	20	308	11	95	16	1800	no brackets	28.0	45	7.7
16	L	20	308	11	95	16	2700	no brackets	28.0	45	5.98
17	L	20	308	11	95	16	3000	no brackets	28.0	45	5.45
18	L	20	308	8	95	16	2400	no brackets	38.5	45	5.39
19	L	11	308	11	95	11	2400	no brackets	28.0	45	5.64

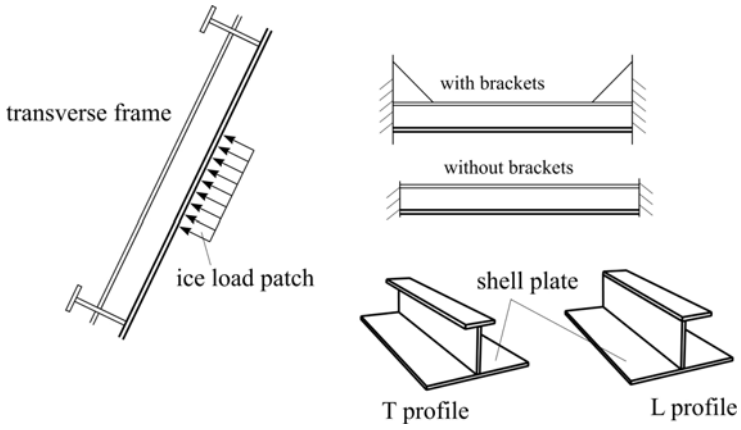

Figure 16. Sketch of transverse frame geometry.

Table 4 shows transverse frames with the same capacity 5.3 MPa according UR formulae analyzed with the patch load length 400 mm and breadth equal to stiffener spacing. All the frames are L sections without brackets and the main variants are web thickness and height, plate thickness flange thickness and frame length.

Table 4. Transverse frame (5.3 MPa capacity) parameters

Run No.	Plate thk. [mm]	Web height [mm]	Web thk. [mm]	Flange width [mm]	Flange thk. [mm]	Frame length [mm]	hw / tw	805 $/(\sigma_y)^{0.5}$
1	10	308	8	95	16	2400	39	45
2	8	308	10	95	12	2400	31	45
3	11	308	10	95	11	2400	31	45
4	7	308	8	95	17	2400	39	45
5	19	308	8	95	15	2400	39	45
6	20	275	9	95	18	2400	31	45
7	20	250	11	95	18	2400	23	45
8	7	308	8	95	18	2000	39	45

5.2 Load-Deflection Results

Transverse frames were loaded until total midspan deformation reached 10% of the stiffener length. As with the longitudinal frames analysis the load–deflection curves show the main results. Two groups of analysis were done:

1. With web height and flange breadth fixed, the main variants were: web, plate and flange thickness, frame length and presence or absence of brackets. These variations are listed in Table 3. Figure 17 shows all the plots for the frames listed in Table 3. Figure 18 shows the results for just the tee frames. Figure 19 shows just the results for the L frames with brackets. Figure 21 shows just the results for L frames without brackets.

2. With the target capacity according UR formulae set to 5.3 MPa, web height, web thickness and plate thickness were varied to achieve similar strength levels. The intention was to investigate how the parameters effected frames capacity. These variations are listed in Table 4. Figure 21 shows all the plots for the frames listed in Table 4.

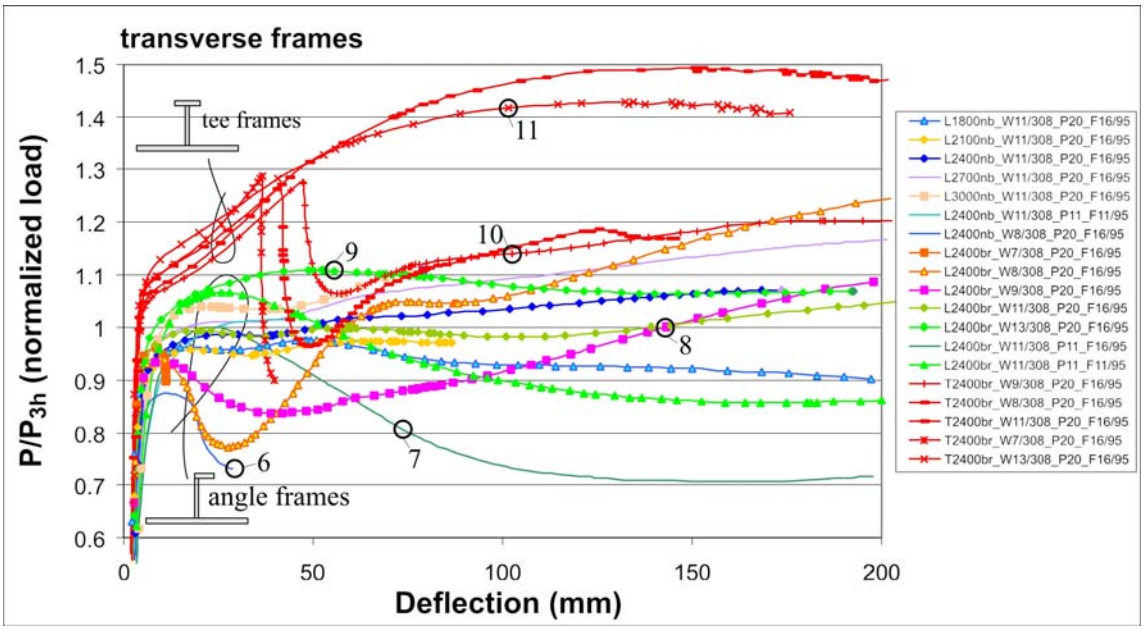

Figure 17. Transverse frames: normalized load–deflection curves

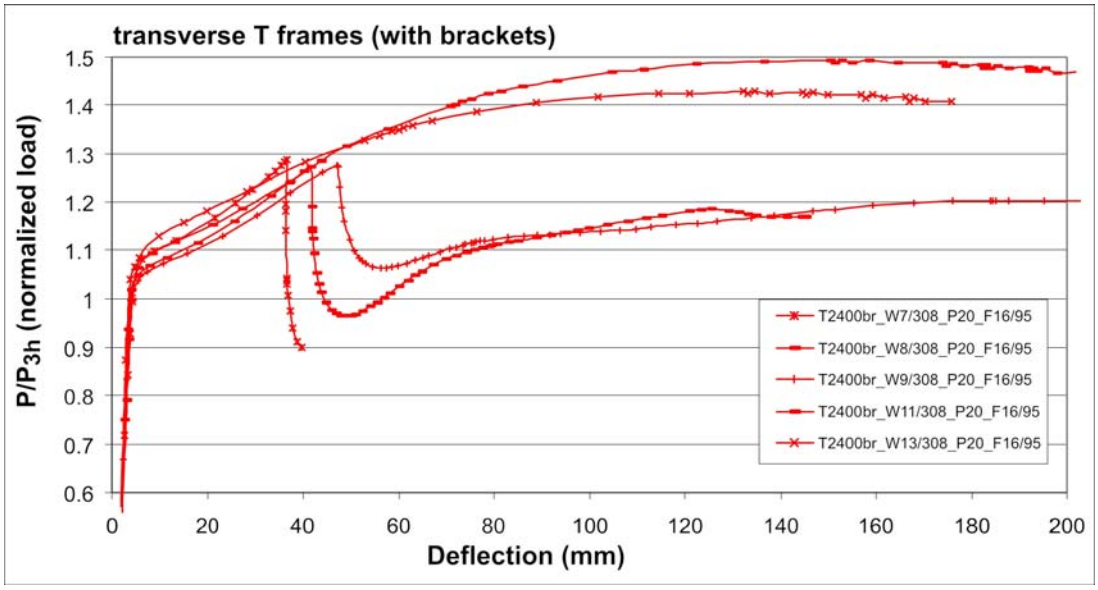

Figure 18. Transverse T frames: normalized load–deflection curves

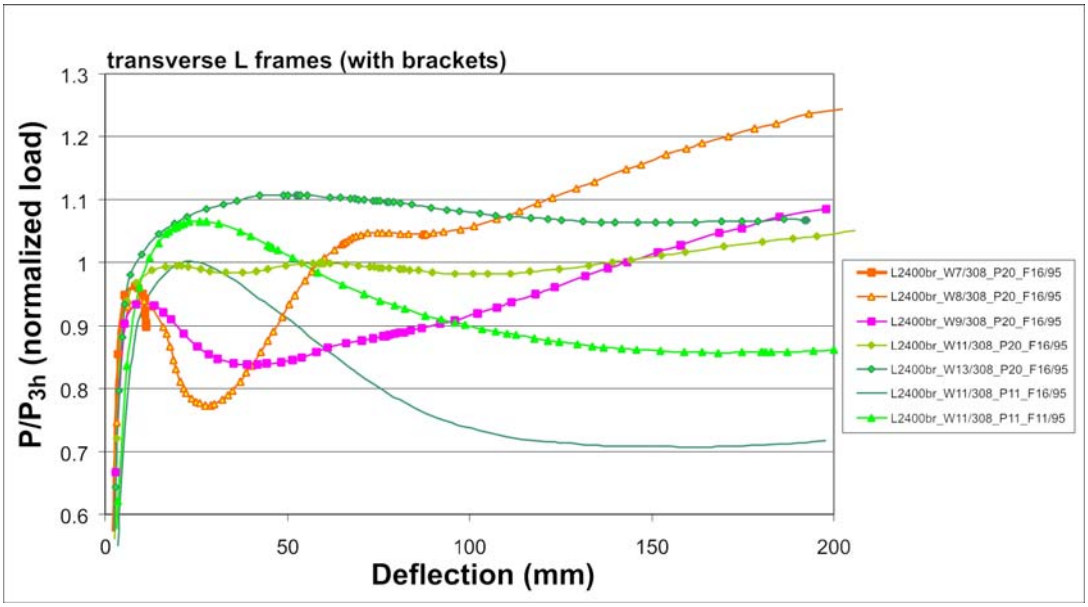

Figure 19. Transverse L frames with brackets : normalized load–deflection curves

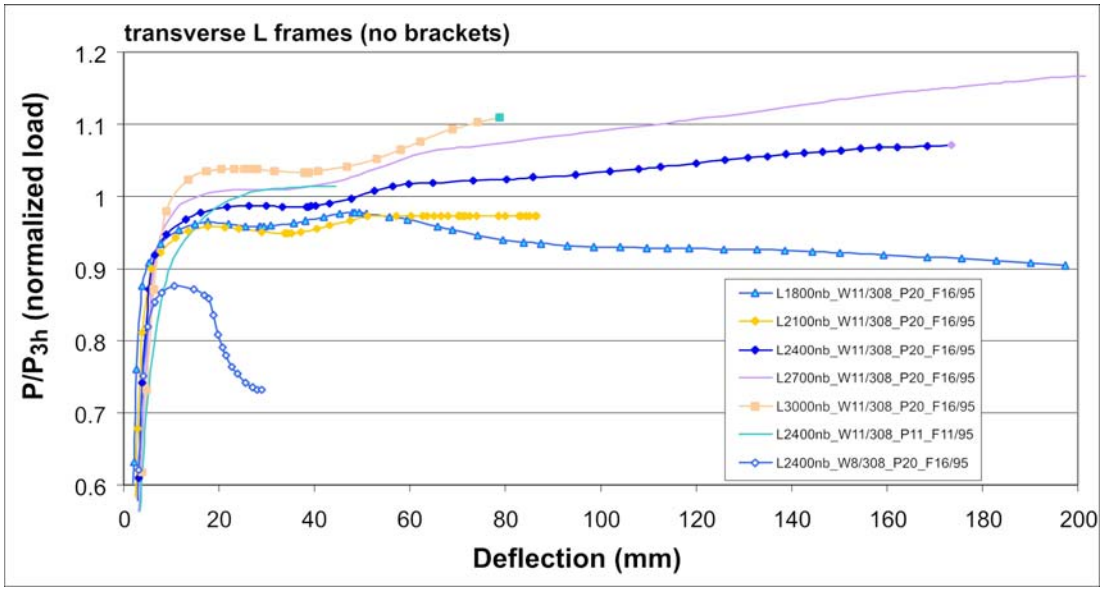

Figure 20. Transverse L frames without brackets : normalized load–deflection curves

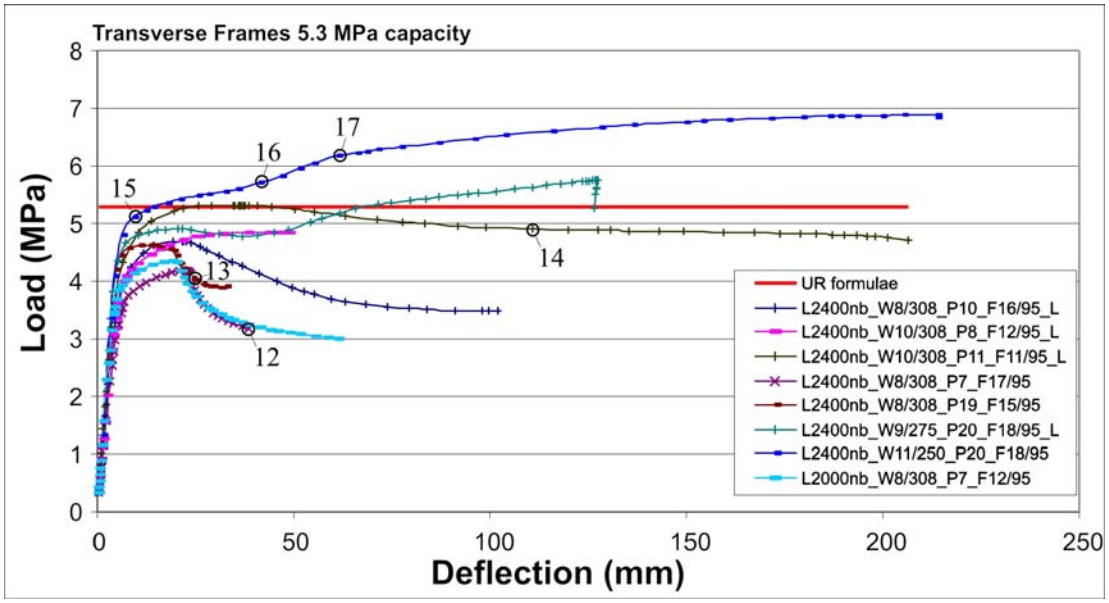

Figure 21. Transverse frames 5.3 MPa capacity: load – deflection curves

5.3 Deformation Plots

The plots shown below show the deformation pattern at the points indicated by the numbered circles in Figure 17 and Figure 21.

Table 5. Table of ANSYS plots (plot number corresponds with circle numbers on the Figure 17 and Figure 21 load deflection curves)

Circle No.	Frame type	Frame dimensions (mm)	Frame length (mm)	Load level (MPa)
6	L transverse	W 8/308_P 20_F 16/95	2400	3.94
7	L transverse	W 11/308_P 11_F 16/95	2400	5.73
8	L transverse	W 9/308_P 20_F 16/95	2400	6.35
9	L transverse	W 13/308_P 20_F 16/95	2400	8.93
10	T transverse	W 9/308_P 20_F 16/95	2400	7.11
11	T transverse	W 13/308_P 20_F 16/95	2400	11.43
12	L transverse	W 8/308_P 7_F 17/95	2400	3.19
13	L transverse	W 8/308_P 19_F 15/95	2400	4.15
14	L transverse	W 10/308_P 11_F 11/95	2400	4.91
15	L transverse	W 11/250_P 20_F 18/95	2400	5.12
16	L transverse	W 11/250_P 20_F 18/96	2400	5.71
17	L transverse	W 11/250_P 20_F 18/97	2400	6.25

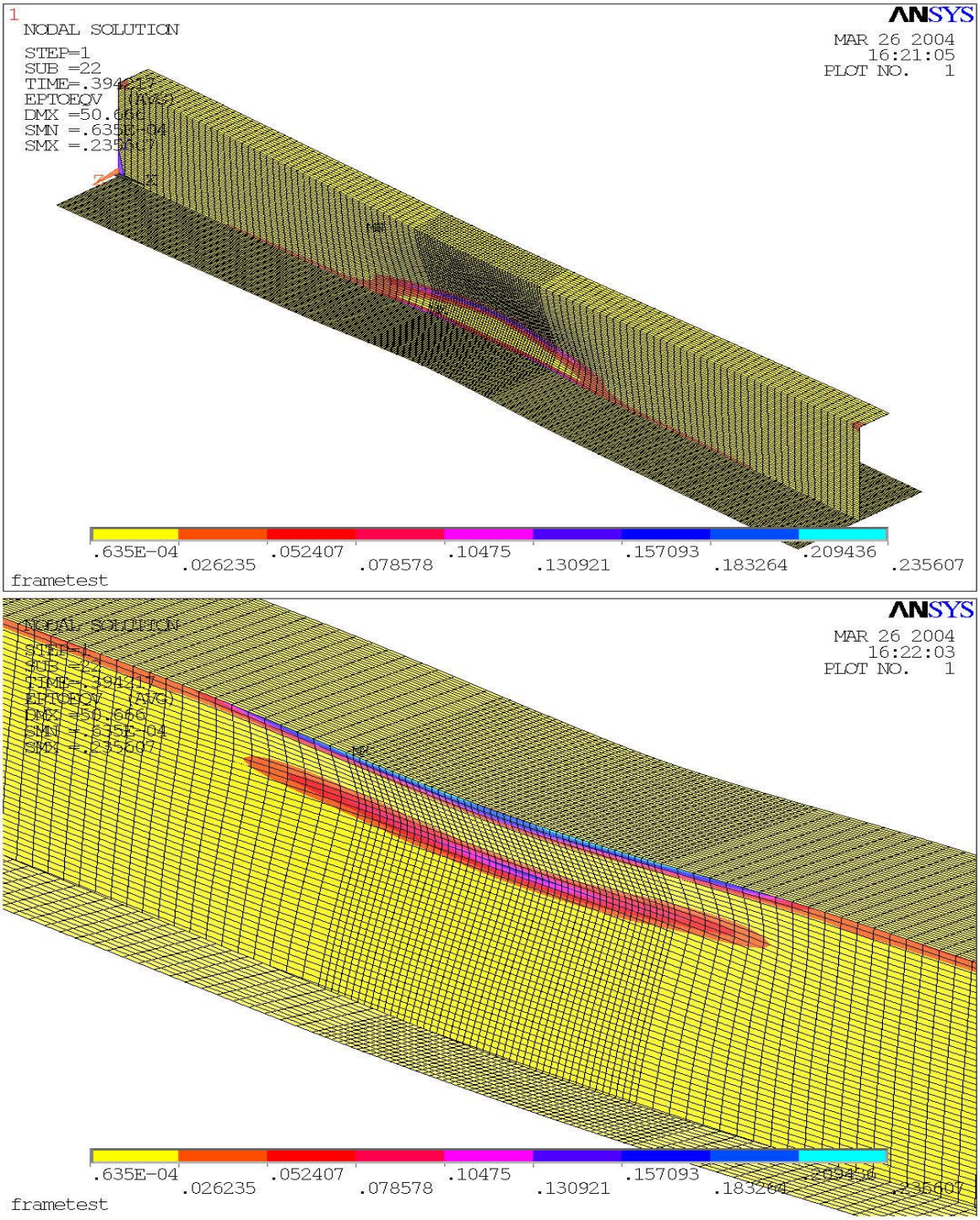

Figure 22. Plot of deformation (with strain contours) for circle #6.

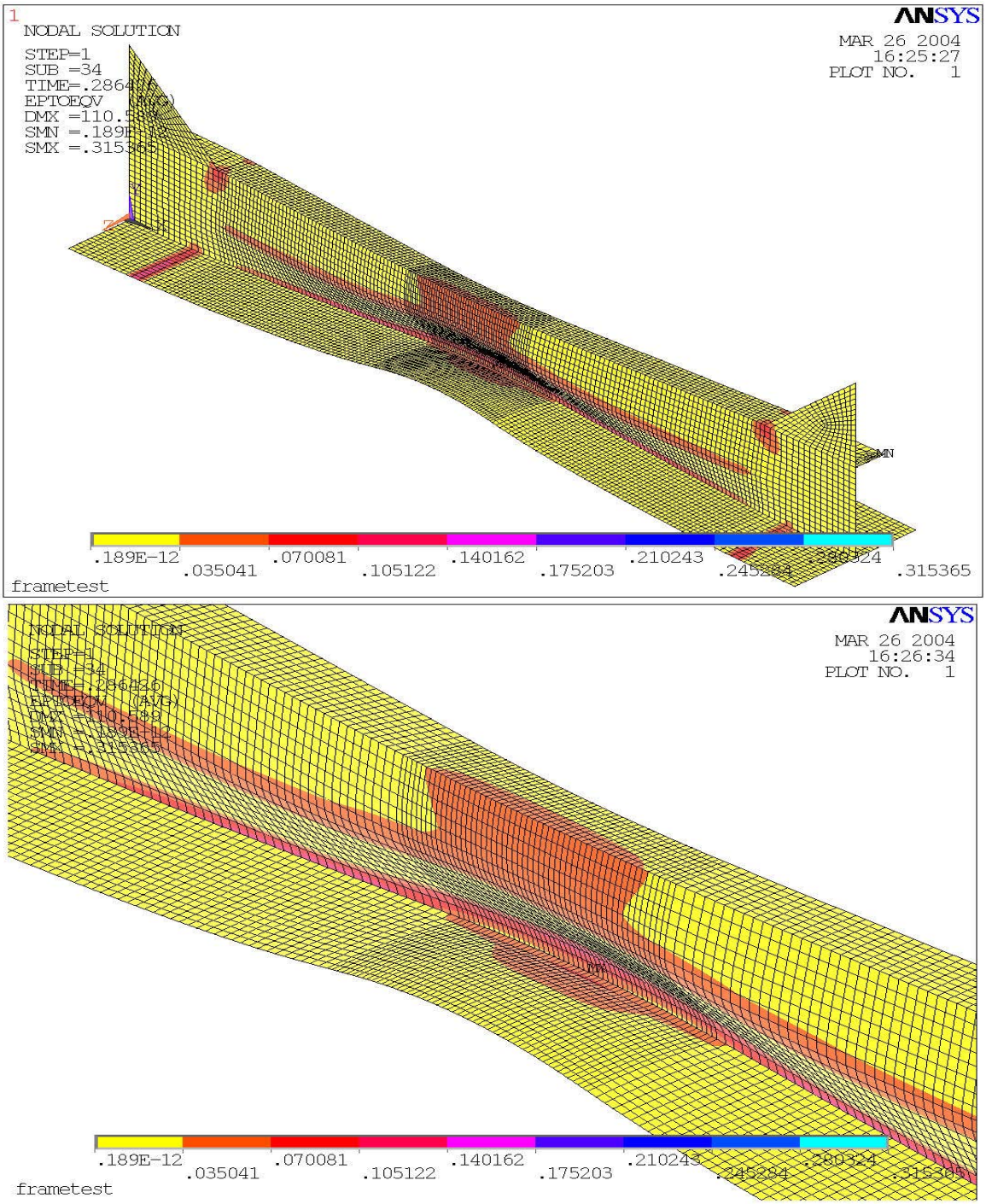

Figure 23. Plot of deformation (with strain contours) for circle #7.

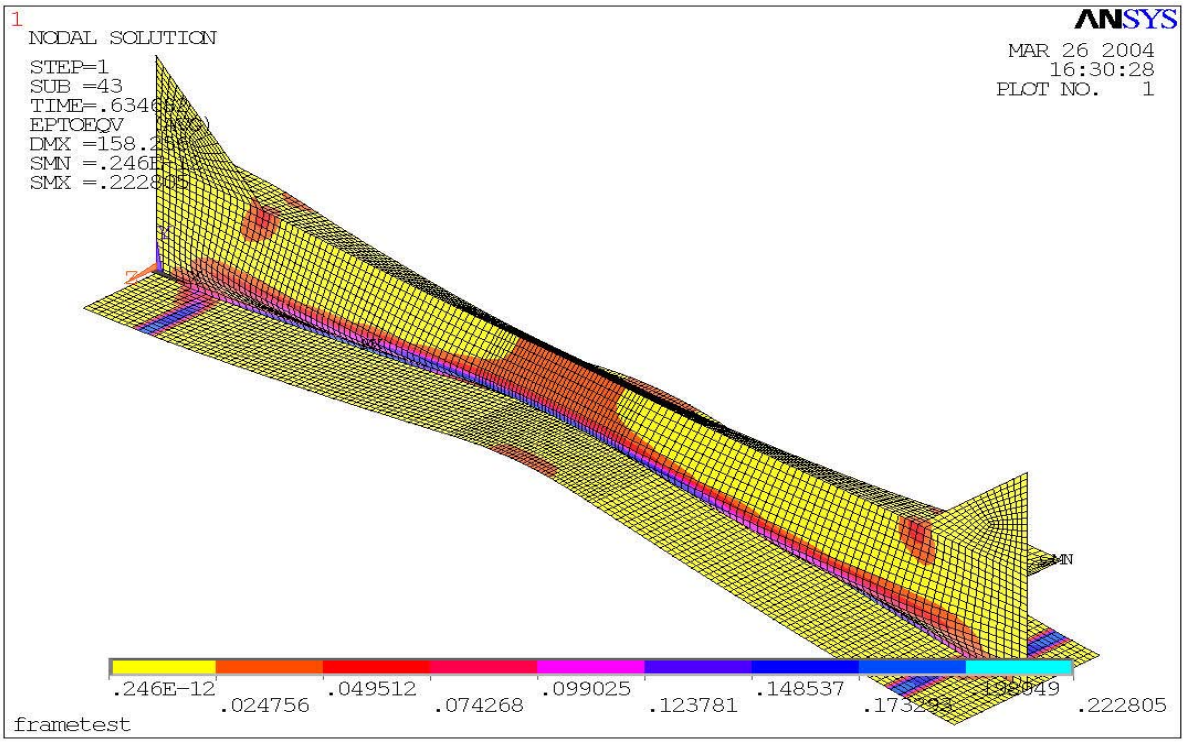

Figure 24. Plot of deformation (with strain contours) for circle #8.

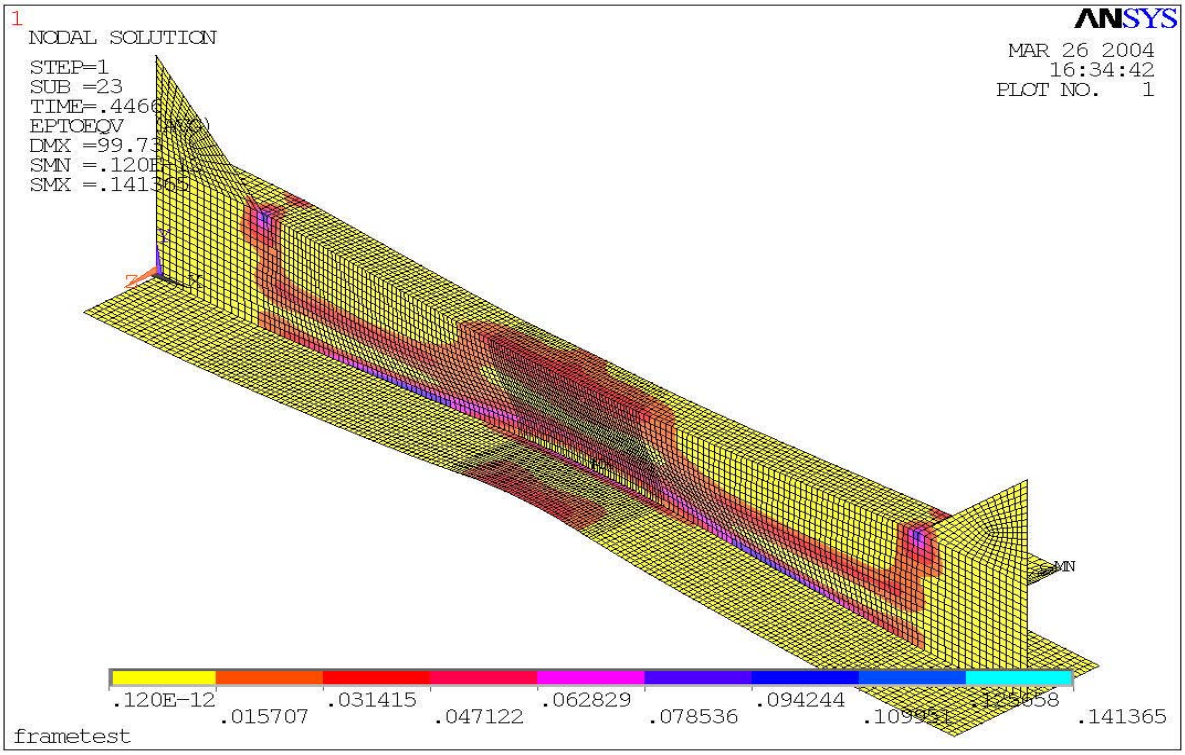

Figure 25. Plot of deformation (with strain contours) for circle #9.

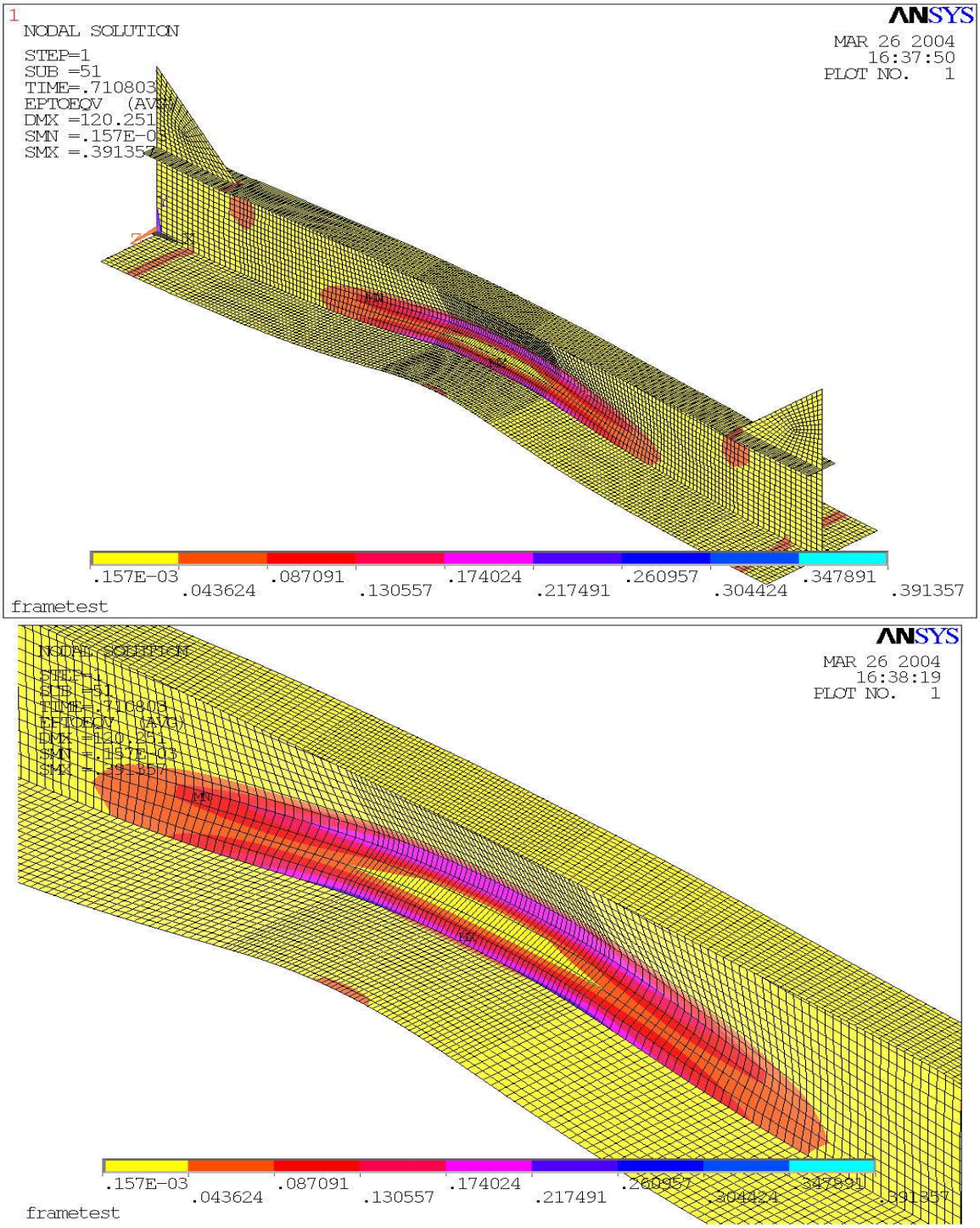

Figure 26. Plot of deformation (with strain contours) for circle #10.

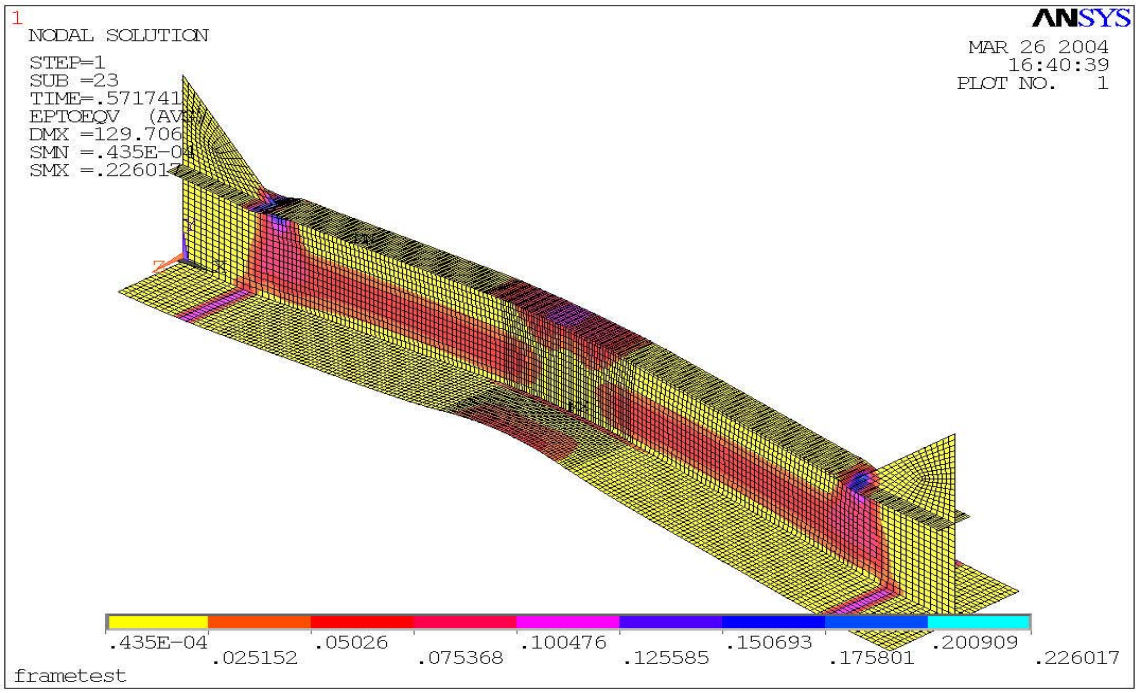

Figure 27. Plot of deformation (with strain contours) for circle #11.

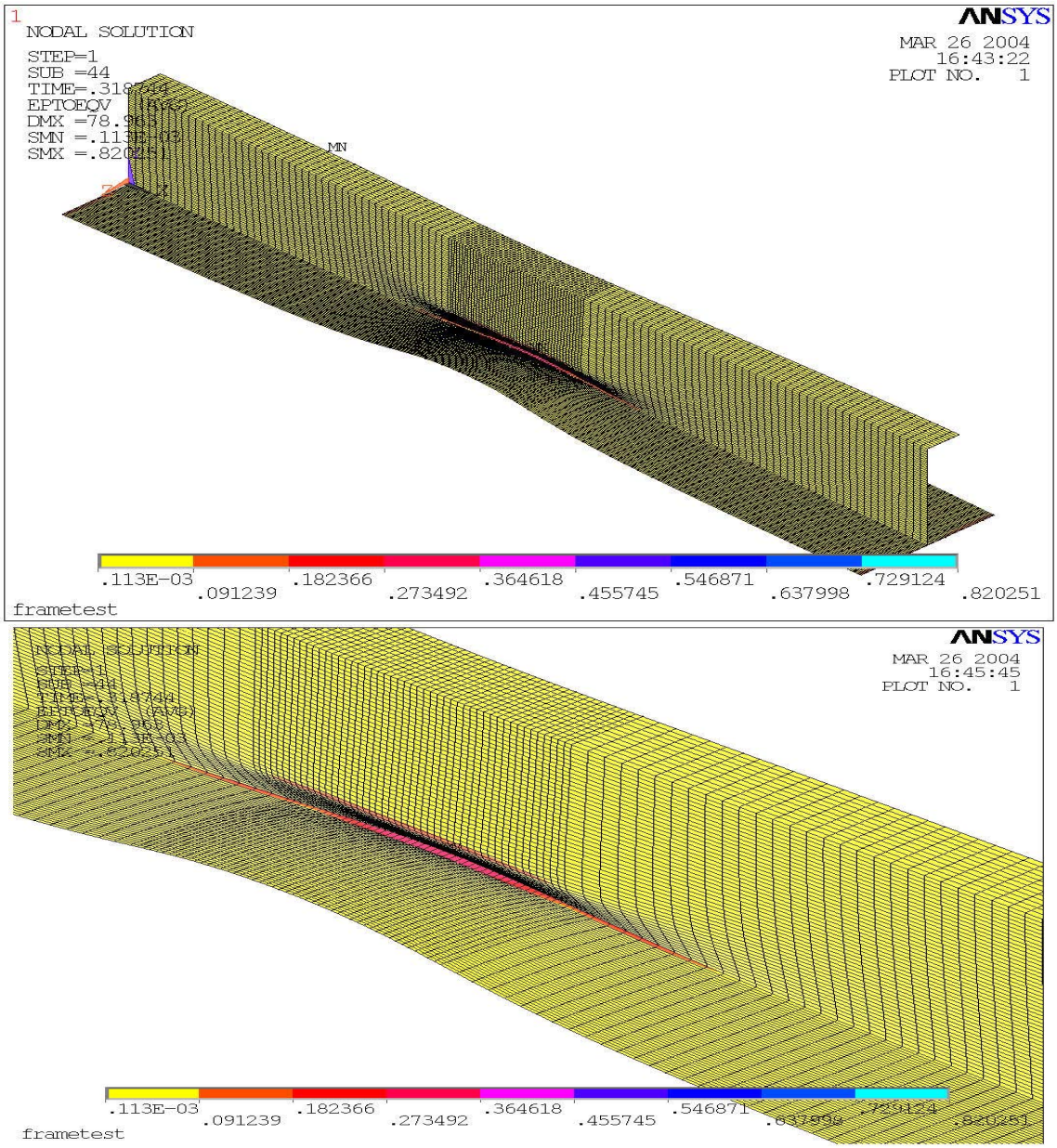

Figure 28. Plot of deformation (with strain contours) for circle #12.

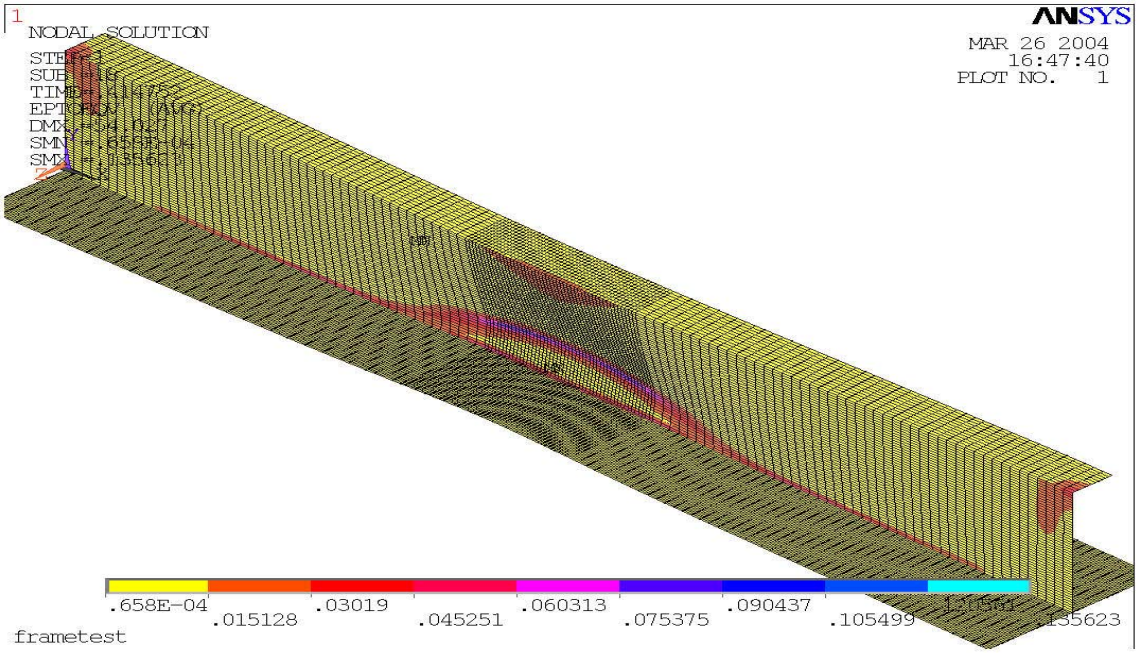

Figure 29. Plot of deformation (with strain contours) for circle #13.

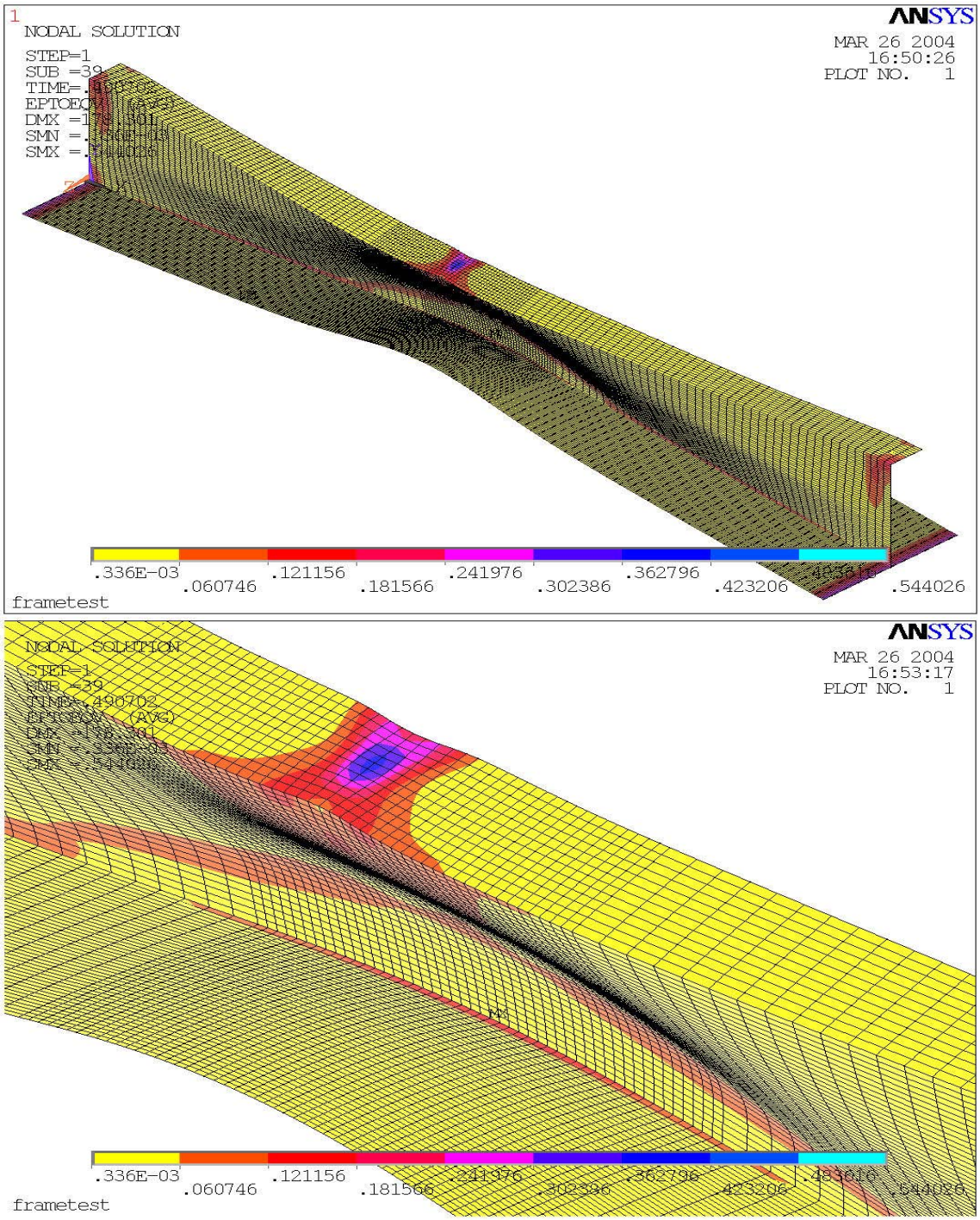

Figure 30. Plot of deformation (with strain contours) for circle #14.

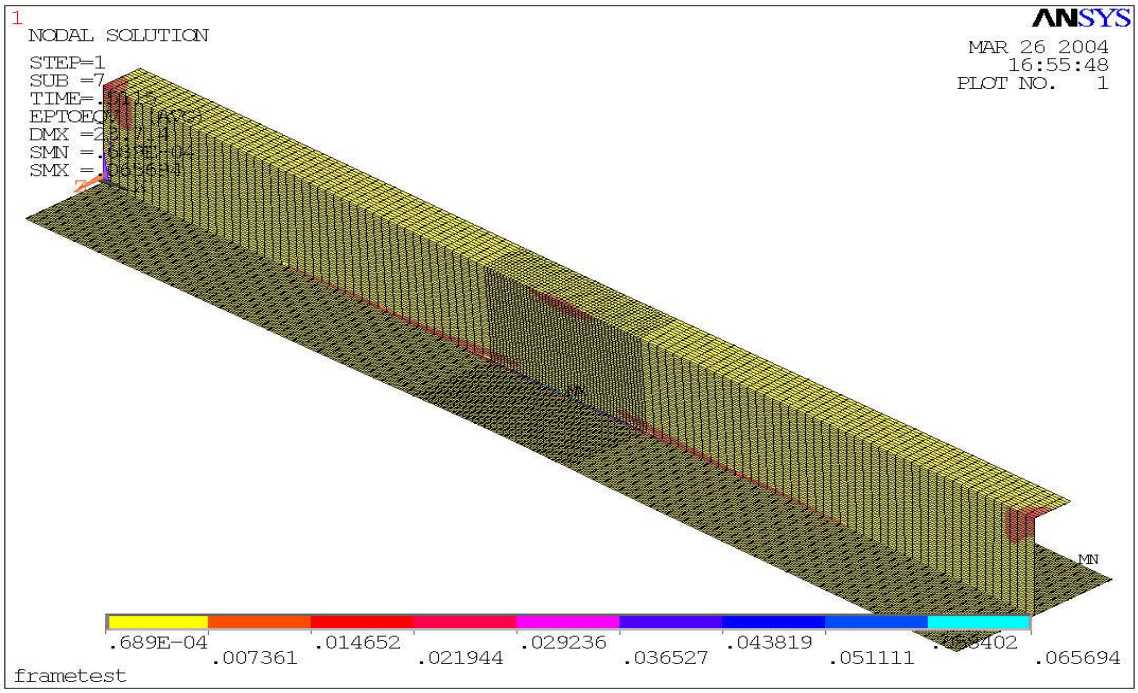

Figure 31. Plot of deformation (with strain contours) for circle #15.

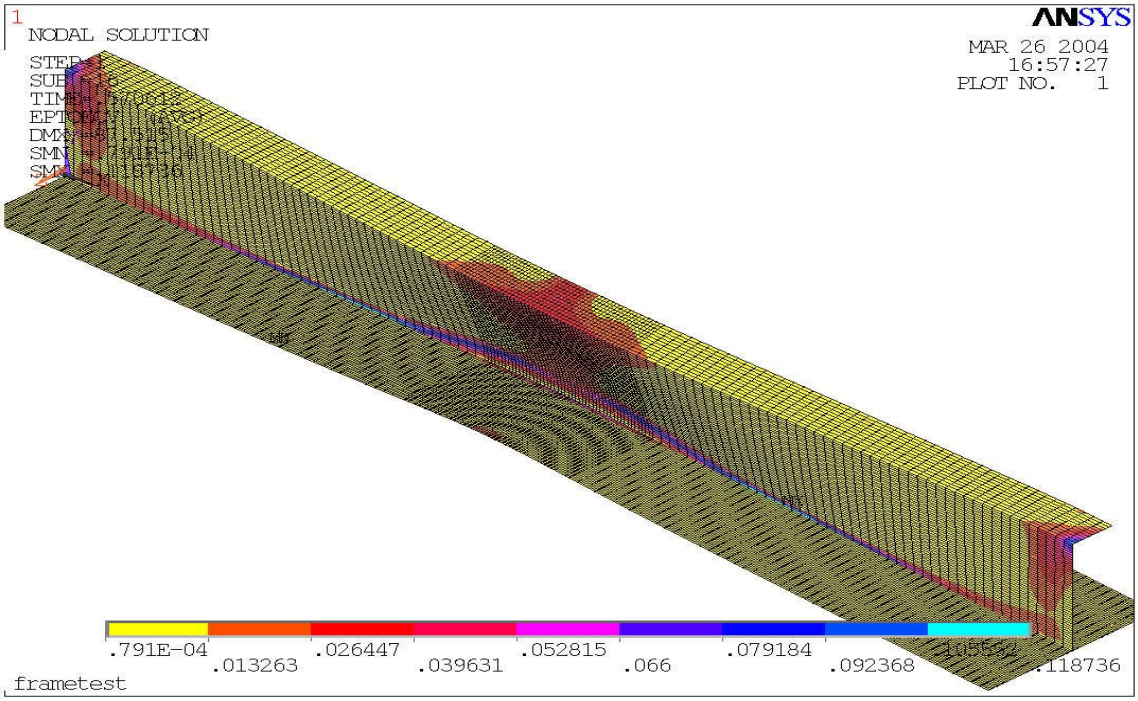

Figure 32. Plot of deformation (with strain contours) for circle #16.

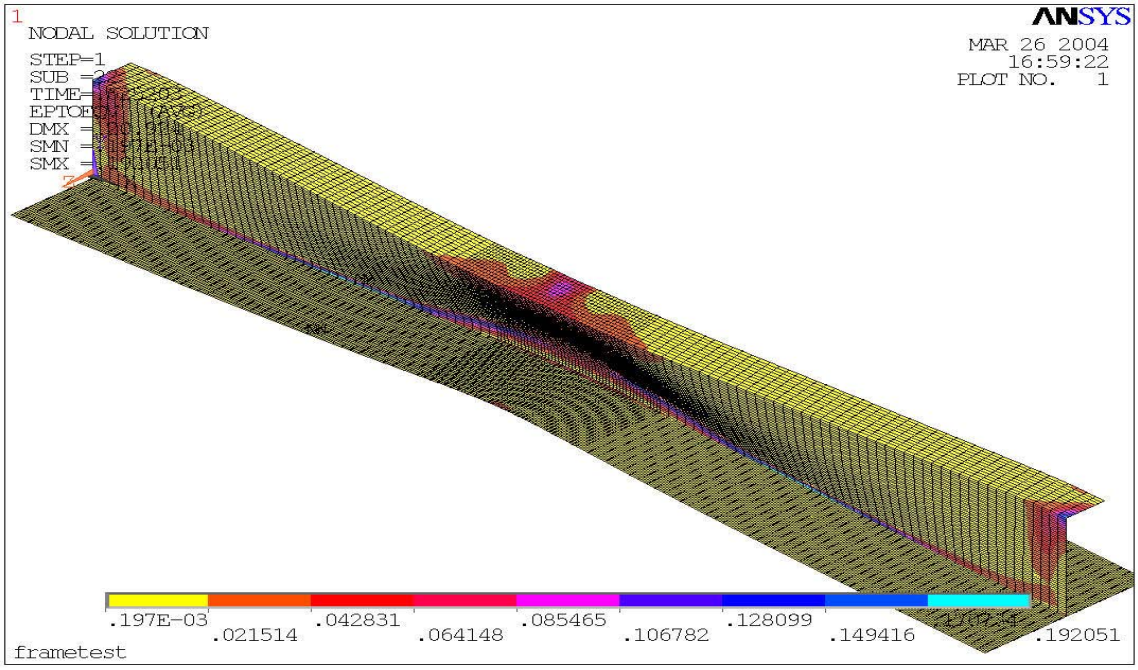

Figure 33. Plot of deformation (with strain contours) for circle #17.

5.4 Discussion of Transverse Frame Results

The load–deflection curves in Figure 17 show that web height, web thickness and flange thickness affect the stiffener behavior. Local buckling deformations in the web directly under the load can provoke rapid stiffener collapse. This seems to be more serious than shear buckling deformations seen in the longitudinal frames.

Figure 18 shows only T frames. Sudden loss of capacity is observed in frames with hw/tw ratio more then 28. The likely cause of the capacity drop is local web buckling at the stiffener midspan area, directly under the load. This type of buckling is similar to elastic buckling (i.e. rapid rather than progressive) and is more dangerous than the shear buckling in the longitudinal frames.
Figure 19 and Figure 20 show only L frames. Similarities to longitudinal frames can be observed. Frames with brackets can have more sudden capacity drops, while longer frames have smoother load-deflection curves. The reason for the sudden drops is the same as for the T frames.

Figure 21 shows transverse frames with the same required capacity 5.3MPa, but with different frame parameters. The frames with thin tall webs and thick flanges have the worst qualitative behavior.

6 Conclusions

The work presented here focuses on behaviour of L and T frames subject to both uniform and patch loads. In particular, the validity of the a limit state equation used in the new IACS Unified Requirements for Polar Ships is under investigation. That equation, (for 3-hinge collapse) was derived on the basis of plastic mechanisms, and by assuming that local buckling would not play a significant part on the collapse. It was assumed that the local buckling requirements in the rules (i.e. limitations on web height to thickness ratio) would ensure that local buckling did not occur, even during and after the formation of the plastic mechanism. The UR does not contain any explicit tripping requirements. This work was also intended to examine the possible need for tripping requirements, with particular attention to angle (L) sections with brackets.

When considering the plastic response of frames, there is no single result that can be used to describe the behaviour as successful. The ideal frame will behave as those shown in Figure 9. The (nearly) linear behaviour should continue until the load exceed the design capacity, and after the onset of large deformations, the load capacity should continue to rise. Any sharp drop in capacity, especially if that results in a drop below the design capacity, is not good. Such sharp drops would likely result in a very rapid and large deformation, with increased potential for fracture.

The results do not show a need for tripping requirements. In cases where the full flange has fallen over (what we would call tripping) the deformation occurs progressively, and does not correspond with any abrupt or significant loss of capacity. The progressive deformations allow the membrane stresses to take up the load, and enable the frame to show considerable reserve.

The results do suggest the need for modifications of the local bucking requirements. In cases of relatively thin webs, the frame capacity can drop suddenly. These drops correspond to local web buckling in either direct compression (in transverse frames under the load), or in shear (at the supports for longitudinal frames).

The sharpest drops occur in T frames, and appear to be exacerbated by large flanges, a result opposite to conventional experience with elastic buckling. This is likely due to the potential for the flange, in the case of plastic deformations, to apply normal load to the web, a circumstance that outweighs the tendency of the flange to stiffen the web.

Both T and L frames experience capacity drops associated with web buckling. The L frames fail more progressively and smoothly, and are often able to mobilize more membrane strength to compensate.

It is clear that the UR limit state is quite valid for most cases. The cases in which the intended frame capacity was not achieved were caused by local bucking. The relative importance of local buckling depends on the type of load (patch or uniform) and the frame type (T,L, flat) and boundary conditions (brackets).

7 Recommendations

1. The desired plastic behaviour has many aspects. It would be very beneficial to develop a clear description and numerical measures of the plastic behaviour. Only with such measures can we properly compare one frame with another. The measures should include a description of initial plastic capacity, size of reserve, and severity of final failure.
2. Local buckling appears to be the biggest potential weakness, leading to loss of plastic capacity. Changes to the local buckling requirements are needed. The difficulty is that the severity of the local buckling problem depends on many aspects, not just the usual local web thickness ratio. The easiest solution would be to change the constant in the local buckling rules from 805 to say 400 or 500. However, this would unnecessarily penalize some frames in some situations. A more precise set of requirements would require more thorough investigation and would be complex to implement. It is recommended that local buckling requirements be discussed further.

8 References

1. ANSYS 6.0, Finite Element Program by SAS IP, Inc, 2001
2. IACS UR (Draft) I2 “Structural Requirements for Polar Class Ships”, 30 July, 2003
3. Daley, C., “Review of the Tripping Requirements” Prepared for IACS Ad-hoc Group on Polar Class Ships and Transport Canada, Aug. 2003
4. Kendrick, A., and Daley, C.G., “Background Notes to Derivation and use of Formulations For Framing Design - IACS Unified Requirements for Polar Ships” Prepared for IACS Ad-hoc Group on Polar Class Ships and Transport Canada, January 2000
5. Daley, C.G., (2002), “Derivation of Plastic Framing Requirements for Polar Ships”, Journal of Marine Structures, Elsevier, 15(6) pp 543-559
6. Daley, C.G., (2002), “Application of Plastic Framing Requirements for Polar Ships”, Journal of Marine Structures, Elsevier, 15(6) pp 533-542

Appendix A
Typical ANSYS Input File

Appendix A – Typical ANSYS Input File

Listed below is a typical ANSYS input file. Comments follow exclamation marks '!'. Variable names are given values using the equals sign '='. Commands start with a keyword followed by a comma. (e.g. `et,1,shell181` means 'element type 1 is shell181'). Refer to the ANSYS command language help file for detailed explanation of all commands.

```
/title,frametest
/prep7
!define variables
!units: mm,MPa
L=2400  !frame length
hw=308  !web height
bl=95   !flange width to left
br=0    !flange width to right
s=400   !frame spacing, plate width
tw=11   !web thickness
tp=20   !plate thickness
tf=16   !flange thickness
E=207000 !initial Young's modulus
fy=315  !yield stress
hb=300  !height of bracket
lb=300  !length of bracket
tb=15   !thickness of bracket

!meshing parameters
n1=52
n2=8
n3=2
n4=16
n5=1

!element types, material properties and dimensions
et,1,shell181
ex,1,E          ! elastic modulus is E
nuxy,1,0.3      !poisons ratio is 0.3
tb,bkin,1       !bi-linear stress strain curve is used
tbdata,1,fy,50   ! post-yield modulus is 50 MPa
r,1,tp
et,2,shell181
r,2,tw
et,3,shell181
r,3,tf
et,4,shell181
r,4,tb

!keypoints
n=0
lx=0
k,n+1,lx,-tp/2,-s/2
k,n+2,lx,-tp/2,0
k,n+3,lx,-tp/2,s/2
k,n+4,lx,hw+tf/2,0
k,n+5,lx,hw+tf/2,-bl
k,n+6,lx,hw+tf/2+hb,0
n=6
```

```
lx=lb
k,n+1,lx,-tp/2,-s/2
k,n+2,lx,-tp/2,0
k,n+3,lx,-tp/2,s/2
k,n+4,lx,hw+tf/2,-bl
k,n+5,lx,hw+tf/2,0
n=11
lx=L-lb
k,n+1,lx,-tp/2,-s/2
k,n+2,lx,-tp/2,0
k,n+3,lx,-tp/2,s/2
k,n+4,lx,hw+tf/2,-bl
k,n+5,lx,hw+tf/2,0
n=16
lx=L
k,n+1,lx,-tp/2,-s/2
k,n+2,lx,-tp/2,0
k,n+3,lx,-tp/2,s/2
k,n+4,lx,hw+tf/2,0
k,n+5,lx,hw+tf/2,-bl
k,n+6,lx,hw+tf/2+hb,0

!define lines conecting keypoints
!sizing lines (for mesh density)
n=0
m=0
l,n+1,n+2
lesize,m+1,,,n4
l,n+2,n+3
lesize,m+2,,,n4
l,n+2,n+4
lesize,m+3,,,n4
l,n+4,n+5
lesize,m+4,,,n2
l,n+4,n+6
lesize,m+5,,,n4
l,n+6,n+11
lesize,m+6,,,n4
l,n+1,n+7
lesize,m+7,,,n4
l,n+2,n+8
lesize,m+8,,,n4
l,n+3,n+9
lesize,m+9,,,n4
l,n+4,n+11
lesize,m+10,,,n4
l,n+5,n+10
lesize,m+11,,,n4
n=6
m=11
l,n+1,n+2
lesize,m+1,,,n4
l,n+2,n+3
lesize,m+2,,,n4
l,n+2,n+5
lesize,m+3,,,n4
l,n+5,n+4
```

```
lesize,m+4,,,n2
l,n+1,n+6
lesize,m+5,,,n1
l,n+2,n+7
lesize,m+6,,,n1
l,n+3,n+8
lesize,m+7,,,n1
l,n+4,n+9
lesize,m+8,,,n1
l,n+5,n+10
lesize,m+9,,,n1
n=11
m=20
l,n+1,n+2
lesize,m+1,,,n4
l,n+2,n+3
lesize,m+2,,,n4
l,n+2,n+5
lesize,m+3,,,n4
l,n+5,n+4
lesize,m+4,,,n2
l,n+1,n+6
lesize,m+5,,,n4
l,n+2,n+7
lesize,m+6,,,n4
l,n+3,n+8
lesize,m+7,,,n4
l,n+4,n+10
lesize,m+8,,,n4
l,n+5,n+9
lesize,m+9,,,n4
l,n+5,n+11
lesize,m+10,,,n4

n=16
m=30
l,n+1,n+2
lesize,m+1,,,n4
l,n+2,n+3
lesize,m+2,,,n4
l,n+2,n+4
lesize,m+3,,,n4
l,n+4,n+5
lesize,m+4,,,n4
l,n+4,n+6
lesize,m+5,,,n4

!create area
n=0
a,n+1,n+2,n+8,n+7 !1
a,n+2,n+3,n+9,n+8 !2
a,n+2,n+8,n+11,n+4 !3
a,n+4,n+5,n+10,n+11 !4
a,n+4,n+6,n+11     !5
n=6
a,n+1,n+2,n+7,n+6 !6
a,n+2,n+3,n+8,n+7 !7
```

```
a,n+2,n+7,n+10,n+5 !8
a,n+5,n+4,n+9,n+10 !9
n=11
a,n+1,n+2,n+7,n+6 !10
a,n+2,n+3,n+8,n+7 !11
a,n+2,n+7,n+9,n+5 !12
a,n+5,n+4,n+10,n+9 !13
a,n+5,n+9,n+11     !14

!give areas the appropriate material properties
asel,s,area,,1,2
asel,a,area,,6,7
asel,a,area,,10,11
AATT,1,1,,
asel,all
asel,s,area,,3
asel,a,area,,8
asel,a,area,,12
AATT,1,2,,
asel,all
asel,s,area,,4
asel,a,area,,9
asel,a,area,,13
AATT,1,3,,
asel,all
asel,s,area,,5
AATT,1,4,,
asel,all
asel,s,area,,14
AATT,1,4,,
asel,all
aglue,all
amesh,all
save

!model mesh is done – move to solution phase
/soln
antype,0    !static analysis

!apply boundary conditions
nsel,s,loc,y,-tp/2
nsel,r,loc,z,-s/2
d,all,rotx,0
d,all,roty,0
d,all,uz,0
nsel,all
nsel,s,loc,y,-tp/2
nsel,r,loc,z,s/2
d,all,rotx,0
d,all,roty,0
d,all,uz,0
nsel,all
nsel,r,loc,x,l
d,all,all,0
nsel,all
nsel,r,loc,x,0
d,all,all,0
```

```
nsel,all
save
/soln

! apply external pressures
py=5
sfa,1,,pres,py !pressure in MPa over L X s area
sfa,2,,pres,py !pressure in MPa over L X s area
sfa,6,,pres,py !pressure in MPa over L X s area
sfa,7,,pres,py !pressure in MPa over L X s area
sfa,10,,pres,py !pressure in MPa over L X s area
sfa,11,,pres,py !pressure in MPa over L X s area

!set solution control parameters
antype,static
nlgeom,on
sstif,on
neqit,30
nropt,full,,off
arclen,on
cnvtol,F,,0.01,,1
cnvtol,M,,0.05,,1
ncnv
pred,on,,on
outres,all,all
nsubst,30
save

! perform solution and save all results
solve
save
```

Appendix B
Finite Element Validation Checks

Appendix B – Finite element validation checks

Results (load deflection curves and stresses) presented earlier in the report are true for frames with geometry generated with shell element type and for material with post-yield modulus 50. Numerous finite elements runs are conducted for frames with solid elements and material with post-yield modulus 500. Some of those results are shown in this Appendix. Generally solid element frames have more capacity and better behavior, difference in the load-deflection curves between shell and solid element are shown on the Figure 34

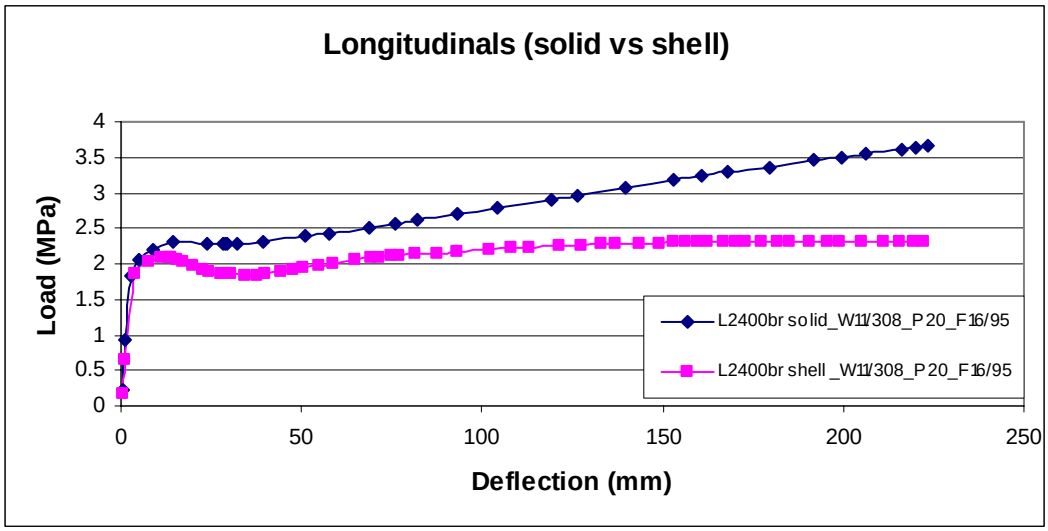

Figure 34. Solid and shell elements comparison plot

Material post-yield modulus difference is shown on Figure 35

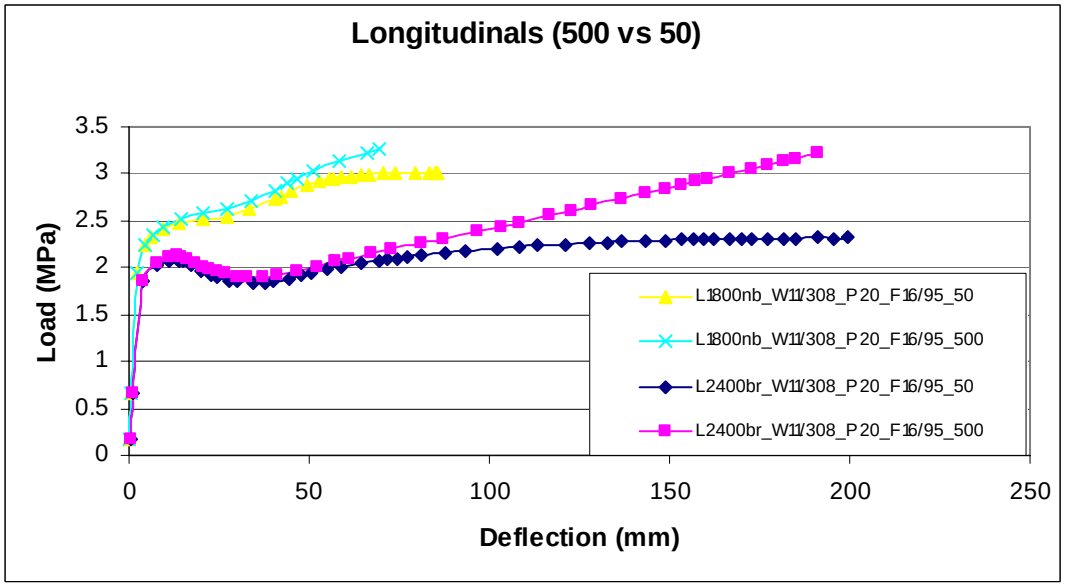

Figure 35. Material post-yield modulus comparison plot

It seems that for the region of interest post-yield modulus has no big influence on the results.

Figure 36shows normalized load – deflection curves for some standard L sections. L sections are analyzed as longitudinal frames, geometry was generated from solid elements and material post yield modulus is 500MPa.

Table 6. Longitudinal frames (solids)

Run No.	Plate thk. [mm]	Web height [mm]	Web thk. [mm]	Flange width [mm]	Flange thk. [mm]	Frame length [mm]	Bracket l x h x t [mm]	hw / tw	805 $/(\sigma_y)^{0.5}$	Capacity by UR formulae (MPa) (eqn 1)
1	12	100	12	65	12	2000	200 X 200 X 12	8	46	0.62
2	8	100	8	65	8	2000	200 X 200 X 8	13	46	0.4
3	11.5	200	11.5	95	15	2000	200 X 200 X 11.5	17	46	1.35
4	11.5	300	11.5	100	16	2000	300 X 300 X 11.5	26	46	1.91
5	12.5	400	12.5	120	25	2000	300 X 300 X 12.5	32	46	2.75
6	11.5	450	11.5	120	25	4000	300 X 300 X 11.5	39	46	1.28
7	13.5	500	13.5	120	35	2000	300 X 300 X 13.5	37	46	3.65
8	11.5	500	11.5	120	30	2000	300 X 300 X 11.5	43	46	3.11
9	11.5	500	11.5	120	30	2000	500 X 500 X 11.5	43	46	3.68
10	11.5	500	11.5	120	35	4000	300 X 300 X 13.5	43	46	1.67

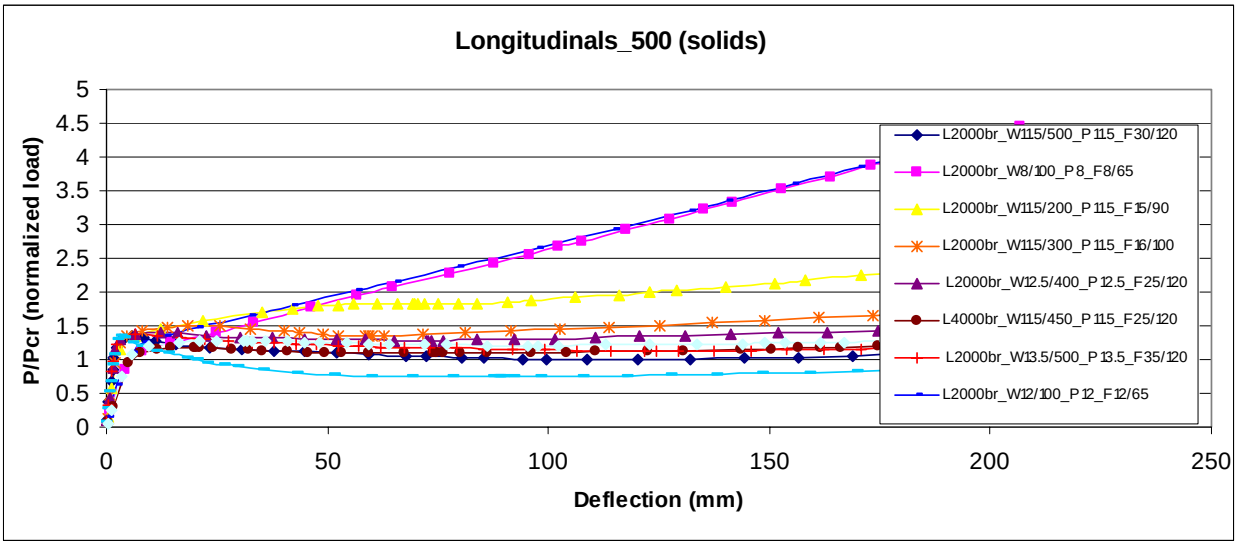

Figure 36. Longitudinal L frames: normalized load–deflection curves